Physics Letters B 780 (2018) 7–20

Contents lists available at ScienceDirect

Physics Letters B

www.elsevier.com/locate/physletb

Search for collectivity with azimuthal J/ψ-hadron correlations in high multiplicity p–Pb collisions at $\sqrt{s_{\rm NN}} = 5.02$ and 8.16 TeV

ALICE Collaboration *

ARTICLE INFO

Article history:
Received 27 September 2017
Received in revised form 14 February 2018
Accepted 14 February 2018
Available online 2 March 2018
Editor: M. Doser

ABSTRACT

We present a measurement of azimuthal correlations between inclusive J/ψ and charged hadrons in p–Pb collisions recorded with the ALICE detector at the CERN LHC. The J/ψ are reconstructed at forward (p-going, $2.03 < y < 3.53$) and backward (Pb-going, $-4.46 < y < -2.96$) rapidity via their $\mu^+\mu^-$ decay channel, while the charged hadrons are reconstructed at mid-rapidity ($|\eta| < 1.8$). The correlations are expressed in terms of associated charged-hadron yields per J/ψ trigger. A rapidity gap of at least 1.5 units is required between the trigger J/ψ and the associated charged hadrons. Possible correlations due to collective effects are assessed by subtracting the associated per-trigger yields in the low-multiplicity collisions from those in the high-multiplicity collisions. After the subtraction, we observe a strong indication of remaining symmetric structures at $\Delta\varphi \approx 0$ and $\Delta\varphi \approx \pi$, similar to those previously found in two-particle correlations at middle and forward rapidity. The corresponding second-order Fourier coefficient (v_2) in the transverse momentum interval between 3 and 6 GeV/c is found to be positive with a significance of about 5σ. The obtained results are similar to the J/ψ v_2 coefficients measured in Pb–Pb collisions at $\sqrt{s_{\rm NN}} = 5.02$ TeV, suggesting a common mechanism at the origin of the J/ψ v_2.

© 2018 The Author. Published by Elsevier B.V. This is an open access article under the CC BY license (http://creativecommons.org/licenses/by/4.0/). Funded by SCOAP[3].

1. Introduction

The measurement of angular correlations between particles produced in hadron and nucleus collisions is a powerful tool to study the particle production mechanisms. Usually the two-particle correlation function is expressed in terms of differences in the azimuthal angle ($\Delta\varphi$) and pseudorapidity ($\Delta\eta$) of the emitted particles. In minimum-bias proton–proton (pp) collisions, the dominant structures in the correlation function are a near-side peak at $(\Delta\varphi, \Delta\eta) \approx (0, 0)$ and an away-side ridge located at $\Delta\varphi \approx \pi$ and elongated in $\Delta\eta$ [1]. The near-side peak originates from jet fragmentation, resonance decays and femtoscopic correlations. The away-side ridge results from fragmentation of recoil jets. In collisions of heavy ions, the two-particle correlation function exhibits additional long-range structures elongated in $\Delta\eta$ [2]. These structures are usually interpreted as signatures of collective particle flow produced during the hydrodynamic evolution of the fireball. They are analyzed in terms of the Fourier coefficients of the relative angle distributions. Assuming factorization, these coefficients are then related to the Fourier coefficients ($v_{\rm n}$) of the particle azimuthal distribution relative to the common symmetry plane of the colliding nuclei's overlap area.

The discovery of a near-side ridge in high-multiplicity pp [3] and p–Pb [4] collisions has increased the interest in two-particle angular correlations in small collision systems. These discoveries were followed by the observation that the near-side ridge in p–Pb collisions is accompanied by an away-side one [5,6]. Long-range structures have also been reported in two-particle correlations in d–Au collisions at RHIC [7,8]. Further studies using multi-particle correlations have proven that the observed long-range correlations are of a collective origin [9–11]. Moreover, the transverse-momentum and particle-mass dependencies of the $v_{\rm n}$ coefficients in p–Pb collisions have been found to be similar to those measured in A–A collisions, suggesting a common hydrodynamic origin of the observed correlations [12,13]. Alternative interpretations, including Color-Glass Condensate based models [14] and final-state parton–parton scattering [15], have also been proposed. Long-range correlations of forward and backward muons with mid-rapidity hadrons have also been found in p–Pb collisions at a center-of-mass energy per nucleon pair $\sqrt{s_{\rm NN}} = 5.02$ TeV [16]. The results show that these correlations persist across wide rapidity ranges and extend into the high muon transverse-momentum interval, which is dominated by decays of heavy flavors.

In pp collisions, the J/ψ resonance is formed mainly from pairs of c and $\bar{\rm c}$ quarks produced in hard scattering reactions during the initial stage of the collision. The theoretical models describing the

* *E-mail address:* alice-publications@cern.ch.

https://doi.org/10.1016/j.physletb.2018.02.039
0370-2693/© 2018 The Author. Published by Elsevier B.V. This is an open access article under the CC BY license (http://creativecommons.org/licenses/by/4.0/). Funded by SCOAP[3].

J/ψ production combine calculations of the production of c$\bar{\text{c}}$ pairs within a perturbative Quantum Chromodynamics approach with the subsequent non-perturbative formation of the c$\bar{\text{c}}$ bound state [17]. In p–Pb collisions, the production is affected by the modification of parton distribution functions inside the nucleus [18] as well as possible energy loss and inelastic scattering inside nuclear matter [19,20]. In A–A collisions, there are two additional competing phenomena that influence the J/ψ production. First is the suppressed production due to the dissociation of the c$\bar{\text{c}}$ pairs in the quark–gluon plasma [21]. Second is the J/ψ enhancement via recombination of charm quarks thermalized in the medium [22,23]. The recombination is expected to become prevalent in central collisions at the LHC energies.

Recently, the ALICE Collaboration has published a precise measurement of the second-order Fourier coefficient, v_2, of the azimuthal distribution of the J/ψ production in Pb–Pb collisions at $\sqrt{s_{\text{NN}}} = 5.02$ TeV [24]. The results show significant v_2 in central and semi-central collisions. The measured J/ψ v_2 at low and intermediate transverse momentum can be qualitatively described by a transport model in which the J/ψ azimuthal anisotropy is inherited from that of recombined charm quarks [25,26]. However, at higher transverse momentum the data still indicates significant v_2 while the transport model predicts significantly smaller values coming mostly from path-length dependent suppression in the almond-shaped interaction region of the colliding nuclei and from non-prompt J/ψ produced from b-hadron decays assuming thermalized b quarks. Given these results in Pb–Pb collisions, it is of interest to study the J/ψ-hadron azimuthal correlations also in the smaller p–Pb system. The recombination of charm quarks, if any, should have much smaller impact, due to the smaller number of initially produced charm quarks with respect to Pb–Pb collisions. The small system size should not lead to a sizeable path-length dependent suppression. Nevertheless, the study of the J/ψ-hadron azimuthal correlations could allow to determine whenever J/ψ production is affected by the medium possibly created in these collisions [27–29].

In this Letter, we present results for long-range correlations between forward (p-going, $2.03 < y < 3.53$) and backward (Pb-going, $-4.46 < y < -2.96$) inclusive J/ψ and mid-rapidity charged hadrons in p–Pb collisions at $\sqrt{s_{\text{NN}}} = 5.02$ and 8.16 TeV. Inclusive J/ψ refers to both prompt J/ψ (direct and decays from higher mass charmonium states) and non-prompt J/ψ (feed down from b-hadron decays).

2. Experimental setup and data samples

A detailed description of the ALICE apparatus can be found in Ref. [30]. Below, we briefly describe the detector systems essential for the present analysis.

In the following, η and y_{lab} will denote the pseudorapidity and rapidity in the ALICE laboratory system. The muons are reconstructed in the muon spectrometer covering the range of $-4 < \eta < -2.5$. The spectrometer contains a front absorber located between 0.9 and 5 m from the nominal interaction point. The absorber is followed by five tracking stations, each made of two planes of Cathode Pad Chambers. The third station is placed inside a dipole magnet with 3 Tm field integral. The tracking stations are followed by an iron wall with a thickness of 7.2 interaction lengths and two trigger stations, each one consisting of two planes of Resistive Plate Chambers.

The position of the interaction point is obtained using the clusters reconstructed in the Silicon Pixel Detector (SPD) [31,32]. The SPD is located in the central barrel of the ALICE apparatus and operated inside a large solenoidal magnet providing a uniform 0.5 T magnetic field parallel to the beam line. The SPD consists of two cylindrical layers which cover $|\eta| < 2.0$ and $|\eta| < 1.4$ with respect to the nominal interaction-point, for the inner and outer layer, respectively. The associated charged hadrons at mid-rapidity are reconstructed via the so-called SPD tracklets, short track segments formed from the clusters in the two layers of the SPD and the primary vertex [32].

The V0 detector [33] consists of two rings of 32 scintillator counters each, covering $2.8 < \eta < 5.1$ (V0-A) and $-3.7 < \eta < -1.7$ (V0-C), respectively. It is used for triggering and event-multiplicity estimation.

The data samples presented here were collected during the 2013 and 2016 p–Pb LHC runs. The collision energy was $\sqrt{s_{\text{NN}}} = 5.02$ and 8.16 TeV for the 2013 and 2016 data samples, respectively. Part of the 5.02 TeV data were collected during the 2016 p–Pb run. Data with both beam configurations, namely Pb–nucleus momentum (denoted as Pb–p collisions) or proton momentum (denoted as p–Pb collisions) oriented towards the muon spectrometer, have been analyzed. The asymmetric beam energies, imposed by the two-in-one LHC magnet design, resulted in collisions whose nucleon–nucleon center-of-mass reference system is shifted in rapidity by 0.465 in the direction of the proton beam with respect to the ALICE laboratory system. The data were taken with a trigger that required coincidence of minimum-bias (MB) and dimuon triggers. The MB trigger was provided by the V0 detector requesting a signal in both V0-A and V0-C rings. Its efficiency is found to be about 98% [34]. The dimuon trigger required at least a pair of opposite-sign track segments in the muon trigger system, each with a transverse momentum (p_{T}) above the threshold of the online trigger algorithm. This threshold was set to provide 50% efficiency for muon tracks with $p_{\text{T}} = 0.5$ GeV/c.

The collected data samples of p–Pb and Pb–p collisions at 5.02 TeV (8.16 TeV) correspond to integrated luminosities of 8.1 and 5.8 (8.7 and 12.9) nb^{-1}, respectively. The maximum interaction pile-up probability ranged up to 3% and 8% during 2013 and 2016 data taking, respectively.

3. Event, track and dimuon selection

The beam-induced background is rejected by requiring that the timing signals from both rings of the V0 detector are compatible with particles coming from collision events. Events containing multiple collisions (pile-up) are rejected by requiring one single interaction vertex reconstructed in the SPD and by exploiting the correlation between the number of clusters in the two layers of the SPD and the number of the reconstructed SPD tracklets.

The longitudinal position of the reconstructed primary vertex (z_{vtx}) is required to be within ± 10 cm from the nominal interaction point. The reconstructed SPD tracklets are selected by applying a z_{vtx}-dependent pseudorapidity cut. The cut is adjusted to exclude the contribution from the edges of the SPD where the detector acceptance is low. For example, we select tracklets within $-1.8 < \eta < 0.5$, $-1.3 < \eta < 1.3$ and $-0.5 < \eta < 1.8$ for events with $z_{\text{vtx}} = 10$, 0 and -10 cm, respectively. The contribution from fake and secondary tracklets is reduced by applying a $|\Delta\Phi| < 5$ mrad cut on the difference between the azimuthal angles of the clusters in the two layers of the SPD with respect to the primary vertex. With this cut, the mean p_{T} of the selected charged hadrons is found to be approximately 0.75 GeV/c [16].

The tracks reconstructed in the muon spectrometer are required to emerge at a radial transverse position between 17.6 and 89.5 cm from the end of the front absorber in order to avoid regions with higher material budget. The tracks reconstructed in the tracking chambers are identified as muons by requiring their matching with corresponding track segments in the trigger chambers. Background tracks are removed with a selection on the product of

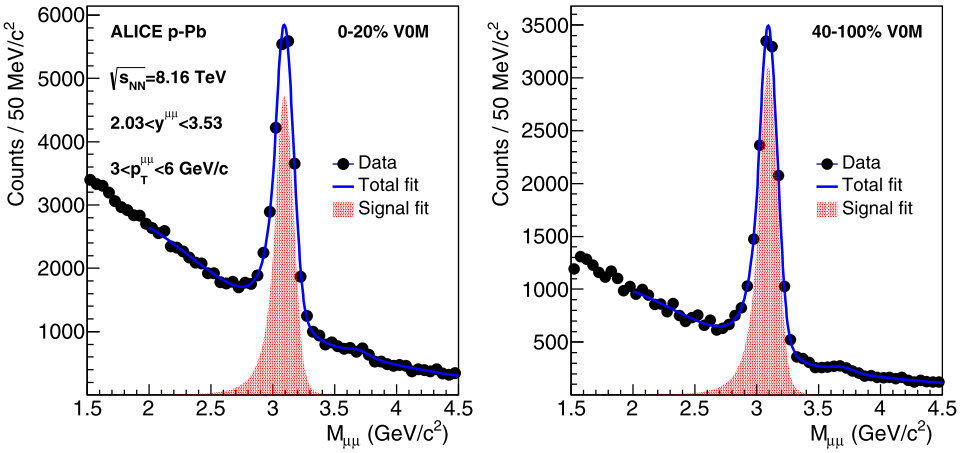

Fig. 1. The $M_{\mu\mu}$ distribution in the $3 < p_{\mathrm{T}}^{\mu\mu} < 6$ GeV/c interval fitted with a combination of a CB2 function for the signal and a VWG function for the background, for high-multiplicity (left panel) and low-multiplicity (right panel) p–Pb collisions at $\sqrt{s_{\mathrm{NN}}} = 8.16$ TeV.

the total track momentum and the distance of closest approach to the primary vertex in the transverse plane [35]. The selected dimuons are defined as pairs of opposite-sign muon tracks having $-4 < y_{\mathrm{lab}}^{\mu\mu} < -2.5$, transverse momentum $p_{\mathrm{T}}^{\mu\mu}$ between 0 and 12 GeV/c and invariant mass $M_{\mu\mu}$ between 1 and 5 GeV/c^2. Only events with at least one dimuon satisfying these selection criteria are considered.

The data samples are split into multiplicity classes based on the total charge deposited in the two rings (V0-A and V0-C) of the V0 detector (V0M) [34]. The high-multiplicity (low-multiplicity) event class is defined as 0–20% (40–100%) of the MB trigger event sample.

4. Analysis

The $M_{\mu\mu}$ distribution in each event-multiplicity class and $p_{\mathrm{T}}^{\mu\mu}$ bin is fit with the combination of an extended Crystal Ball (CB2) function for the J/ψ signal and a Variable-Width Gaussian (VWG) function for the background [36]. The tail parameters of the CB2 function were fixed to the values used in [37,38]. The J/ψ peak position and width were obtained from the fit in the 0–100% event class and fixed to these values in the other event-multiplicity classes. Examples of the $M_{\mu\mu}$ fit in the 0–20% and the 40–100% event classes in the $3 < p_{\mathrm{T}}^{\mu\mu} < 6$ GeV/c interval are shown in Fig. 1.

The angular correlations between J/ψ and charged hadrons are obtained from the associated-particle (SPD tracklets) yields per dimuon trigger. The yields are defined as

$$
\begin{aligned}
&Y^i(z_{\mathrm{vtx}}, M_{\mu\mu}, p_{\mathrm{T}}^{\mu\mu}, \Delta\varphi, \Delta\eta) \\
&= \frac{1}{N^i_{\mathrm{trig}}(z_{\mathrm{vtx}}, M_{\mu\mu}, p_{\mathrm{T}}^{\mu\mu})} \frac{\mathrm{d}^2 N^i_{\mathrm{assoc}}(z_{\mathrm{vtx}}, M_{\mu\mu}, p_{\mathrm{T}}^{\mu\mu})}{\mathrm{d}\Delta\varphi \mathrm{d}\Delta\eta} \\
&= \frac{1}{N^i_{\mathrm{trig}}(z_{\mathrm{vtx}}, M_{\mu\mu}, p_{\mathrm{T}}^{\mu\mu})} \frac{SE^i(z_{\mathrm{vtx}}, M_{\mu\mu}, p_{\mathrm{T}}^{\mu\mu}, \Delta\varphi, \Delta\eta)}{ME^i(z_{\mathrm{vtx}}, M_{\mu\mu}, p_{\mathrm{T}}^{\mu\mu}, \Delta\varphi, \Delta\eta)}, \qquad (1)
\end{aligned}
$$

where $N^i_{\mathrm{trig}}(z_{\mathrm{vtx}}, M_{\mu\mu}, p_{\mathrm{T}}^{\mu\mu})$ is the number of dimuons, $N^i_{\mathrm{assoc}}(z_{\mathrm{vtx}}, M_{\mu\mu}, p_{\mathrm{T}}^{\mu\mu})$ is the number of associated SPD tracklets corrected for acceptance and combinatorial effects (as shown in the second line of the equation and described below), $\Delta\varphi$ and $\Delta\eta = y_{\mathrm{lab}}^{\mu\mu} - \eta_{\mathrm{tracklet}}$ are the azimuthal angle and (pseudo)rapidity difference between the trigger dimuon and the associated SPD tracklet. The yields are calculated separately in each event-multiplicity class (index i) and 1 cm-wide z_{vtx} interval. The distribution

$$
SE^i(z_{\mathrm{vtx}}, M_{\mu\mu}, p_{\mathrm{T}}^{\mu\mu}, \Delta\varphi, \Delta\eta) = \frac{\mathrm{d}^2 N^i_{\mathrm{same}}(z_{\mathrm{vtx}}, M_{\mu\mu}, p_{\mathrm{T}}^{\mu\mu})}{\mathrm{d}\Delta\varphi \mathrm{d}\Delta\eta}
$$

is the yield of associated SPD tracklets from the same event. The distribution

$$
\begin{aligned}
&ME^i(z_{\mathrm{vtx}}, M_{\mu\mu}, p_{\mathrm{T}}^{\mu\mu}, \Delta\varphi, \Delta\eta) \\
&\quad = \alpha^i(z_{\mathrm{vtx}}, M_{\mu\mu}, p_{\mathrm{T}}^{\mu\mu}) \frac{\mathrm{d}^2 N^i_{\mathrm{mixed}}(z_{\mathrm{vtx}}, M_{\mu\mu}, p_{\mathrm{T}}^{\mu\mu})}{\mathrm{d}\Delta\varphi \mathrm{d}\Delta\eta}
\end{aligned}
$$

is constructed using the event-mixing technique, i.e. combining dimuons from one event with SPD tracklets from other events selected in the same event-multiplicity class and z_{vtx} interval. It serves both to correct for detector acceptance and efficiency and to take into account the combinatorial background. The normalization factor $\alpha^i(z_{\mathrm{vtx}}, M_{\mu\mu}, p_{\mathrm{T}}^{\mu\mu})$ is defined as $1/(\mathrm{d}^2 N^i_{\mathrm{mixed}}(z_{\mathrm{vtx}}, M_{\mu\mu}, p_{\mathrm{T}}^{\mu\mu})/\mathrm{d}\Delta\varphi\mathrm{d}\Delta\eta)$ in the $\Delta\eta$ region corresponding to the maximal acceptance [16].

Within each event-multiplicity class and bin of $M_{\mu\mu}$, $p_{\mathrm{T}}^{\mu\mu}$, $\Delta\varphi$ and $\Delta\eta$, the yields Y^i averaged over z_{vtx} are obtained by fitting the distribution $Y^i N_{\mathrm{trig}}(z_{\mathrm{vtx}})^i ME^i(z_{\mathrm{vtx}})$ to the distribution $SE^i(z_{\mathrm{vtx}})$. A Poisson likelihood fit is used in order to properly deal with the cases of low number of tracklets. Then, the average yields are projected on the $\Delta\varphi$ axis in the range of $1.5 < |\Delta\eta| < 5$ using the method described in [16].

In order to extract the yields per J/ψ trigger, the yields per dimuon trigger in each event-multiplicity class, $p_{\mathrm{T}}^{\mu\mu}$ and $\Delta\varphi$ bins are fit as a function of $M_{\mu\mu}$ using the following superposition

$$
Y^i(M_{\mu\mu}) = \frac{S}{S+B} Y^i_{\mathrm{J}/\psi} + \frac{B}{S+B} Y^i_B(M_{\mu\mu}), \qquad (2)
$$

where S and B are the number of J/ψ and the background dimuons in each bin of $M_{\mu\mu}$ obtained from the invariant mass fit (using a CB2 function for the J/ψ signal and a VWG function for the background) described above, $Y_{\mathrm{J}/\psi}$ is the associated yield corresponding to the J/ψ trigger and $Y_B(M_{\mu\mu})$ is a second-order polynomial function aimed to describe the associated yields corresponding to the background. The fit range is chosen between 1.5 and 4.5 GeV/c^2. Examples of fits in high-multiplicity and low-multiplicity event classes are shown in Fig. 2.

Fig. 3 shows the obtained associated tracklet yields per J/ψ trigger for p–Pb and Pb–p collisions at $\sqrt{s_{\mathrm{NN}}} = 5.02$ and 8.16 TeV.

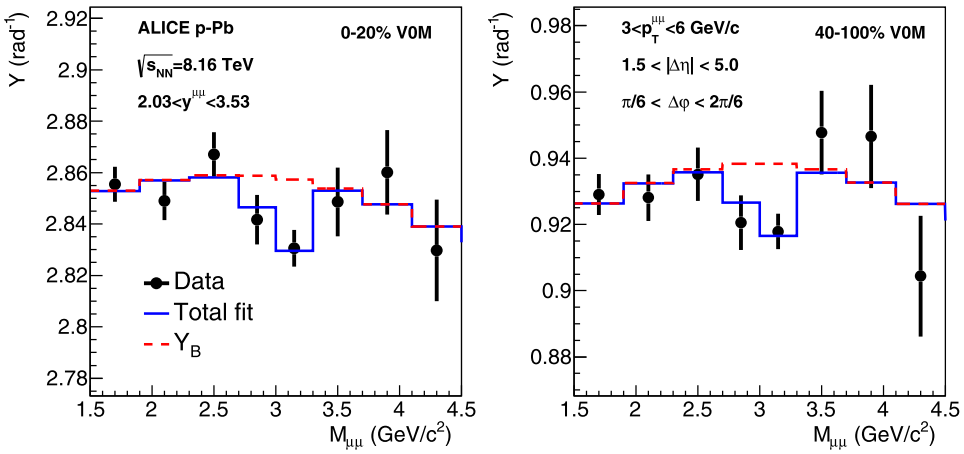

Fig. 2. Example of associated tracklet yields per dimuon trigger in the $3 < p_{\mathrm{T}}^{\mu\mu} < 6$ GeV/c interval for high-multiplicity (left panel) and low-multiplicity (right panel) p–Pb collisions at $\sqrt{s_{\mathrm{NN}}} = 8.16$ TeV. The result of the fit with the function from Eq. (2) is represented with the blue solid line. The dashed red line corresponds to the associated tracklet yields per background dimuon. (For interpretation of the colors in the figure(s), the reader is referred to the web version of this article.)

As expected, in low-multiplicity collisions we observe a significant correlation structure on the away side (Fig. 3, top panels), presumably originating from the fragmentation of recoil jets. In high-multiplicity collisions (Fig. 3, middle panels), a possible enhancement on both near ($\Delta\varphi \approx 0$) and away ($\Delta\varphi \approx \pi$) side can be spotted on top of the away-side structure. In order to isolate possible correlations due to collective effects between the J/ψ and the associated tracklets, we apply the same subtraction method as in previous measurements [5,6,12,16], namely subtracting the $Y_{\mathrm{J}/\psi}$ yields in low-multiplicity collisions from those in high-multiplicity collisions (Fig. 3, bottom panels). The subtraction method relies on the assumptions that the jet correlations on the away side remain unmodified as a function of the event multiplicity and that there are no significant correlations due to collective effects in low-multiplicity collisions (see discussion in Section 6).

In order to quantify the remaining correlation structures, the subtracted yields $Y^{sub}_{\mathrm{J}/\psi}(\Delta\varphi)$ are fit with

$$a_0 + 2a_1 \cos\Delta\varphi + 2a_2 \cos 2\Delta\varphi. \tag{3}$$

The second-order Fourier coefficient $V_2\{\mathrm{J}/\psi - \mathrm{tracklet, sub}\}$ of the azimuthal correlation between the J/ψ and the associated charged hadrons is finally calculated as a_2/b_0^{high}. The denominator $b_0^{\mathrm{high}} = a_0 + b_0^{\mathrm{low}}$ corresponds to the combinatorial baseline of the high-multiplicity collisions, where the parameter b_0^{low} is the combinatorial baseline of the low-multiplicity collisions obtained at the minimum of the per-trigger yields, namely in $\Delta\varphi < \pi/6$. The parameter b_0^{low} is the normalization factor used in Fig. 3. The parameter a_1, which describes the strength of the remaining away-side correlation structure, is found to be compatible with zero in practically all $p_{\mathrm{T}}^{\mathrm{J}/\psi}$ intervals, in both p–Pb and Pb–p collisions at both 5.02 and 8.16 TeV.

As an alternative extraction method, the calculation of b_0^{low}, the subtraction of low-multiplicity from high-multiplicity collision yields and the fit to Eq. (3) is done in each bin of $M_{\mu\mu}$ separately. Then the $V_2\{\mathrm{J}/\psi - \mathrm{tracklet, sub}\}$ coefficient is extracted by fitting $V_2\{\mu\mu - \mathrm{tracklet, sub}\}(M_{\mu\mu})$ with a superposition similar to the one defined in Eq. (2)

$$\begin{aligned} &V_2\{\mu\mu - \mathrm{tracklet, sub}\}(M_{\mu\mu}) \\ &= \frac{S}{S+B} V_2\{\mathrm{J}/\psi - \mathrm{tracklet, sub}\} \\ &\quad + \frac{B}{S+B} V_2^B\{\mu\mu - \mathrm{tracklet, sub}\}(M_{\mu\mu}), \end{aligned} \tag{4}$$

where the $V_2^B\{\mu\mu - \mathrm{tracklet, sub}\}(M_{\mu\mu})$ is the second-order Fourier coefficient of the azimuthal correlation between the background dimuons and associated tracklets. The background coefficient $V_2^B\{\mu\mu - \mathrm{tracklet, sub}\}(M_{\mu\mu})$ is parameterized with a second-order polynomial function. This parameterization is chosen since it reproduces the dimuon $v_2(M_{\mu\mu})$ constructed from the measured muon v_2 coefficient [16] assuming that the dominant part of the background is combinatorial. An example of the $V_2\{\mu\mu - \mathrm{tracklet, sub}\}(M_{\mu\mu})$ fit is shown in Fig. 4.

Following the procedure used in Refs. [5,12,16], the $V_2\{\mathrm{J}/\psi - \mathrm{tracklet, sub}\}$ coefficient is factorized into a product of J/ψ and charged-hadron v_2 coefficients. Thus, the J/ψ second-order Fourier azimuthal coefficient $v_2^{\mathrm{J}/\psi}\{2, \mathrm{sub}\}$ is obtained as

$$v_2^{\mathrm{J}/\psi}\{2, \mathrm{sub}\} = V_2\{\mathrm{J}/\psi - \mathrm{tracklet, sub}\}/v_2^{\mathrm{tracklet}}\{2, \mathrm{sub}\}, \tag{5}$$

where the $v_2^{\mathrm{tracklet}}\{2, \mathrm{sub}\}$ is the tracklet second-order Fourier azimuthal coefficient obtained by performing the analysis considering SPD tracklets as both trigger and associated particles. The obtained values of $v_2^{\mathrm{tracklet}}\{2, \mathrm{sub}\}$ are between 0.067 and 0.069 depending on the beam configuration and collision energy, with 1–2% relative statistical uncertainty and 5–6.5% relative systematic uncertainty.

5. Systematic uncertainties

The combined statistical and systematic uncertainties of the measured $v_2^{\mathrm{tracklet}}\{2, \mathrm{sub}\}$ coefficient for each beam configuration and collision energy are taken as global systematic uncertainties of the corresponding $v_2^{\mathrm{J}/\psi}\{2, \mathrm{sub}\}$ coefficients.

All the other systematic uncertainties of the $v_2^{\mathrm{J}/\psi}\{2, \mathrm{sub}\}$ coefficients are obtained for each data sample and p_{T} interval separately. The following sources are considered.

A possible inaccurate correction for the SPD acceptance is assessed by varying the z_{vtx} range between ± 8 and ± 12 cm. Systematic uncertainties are assigned only in the cases of a significant change of the results. The significance is defined according to the procedure described in Ref. [39].

The systematic effect related to the uncertainty of the shape of the dimuon background yields $Y_B(M_{\mu\mu})$ is estimated by performing the fit with Eq. (2) using a linear function for the background term and varying the fit range. The systematic effect coming from the uncertainty of the signal-to-background ratio S/B is checked

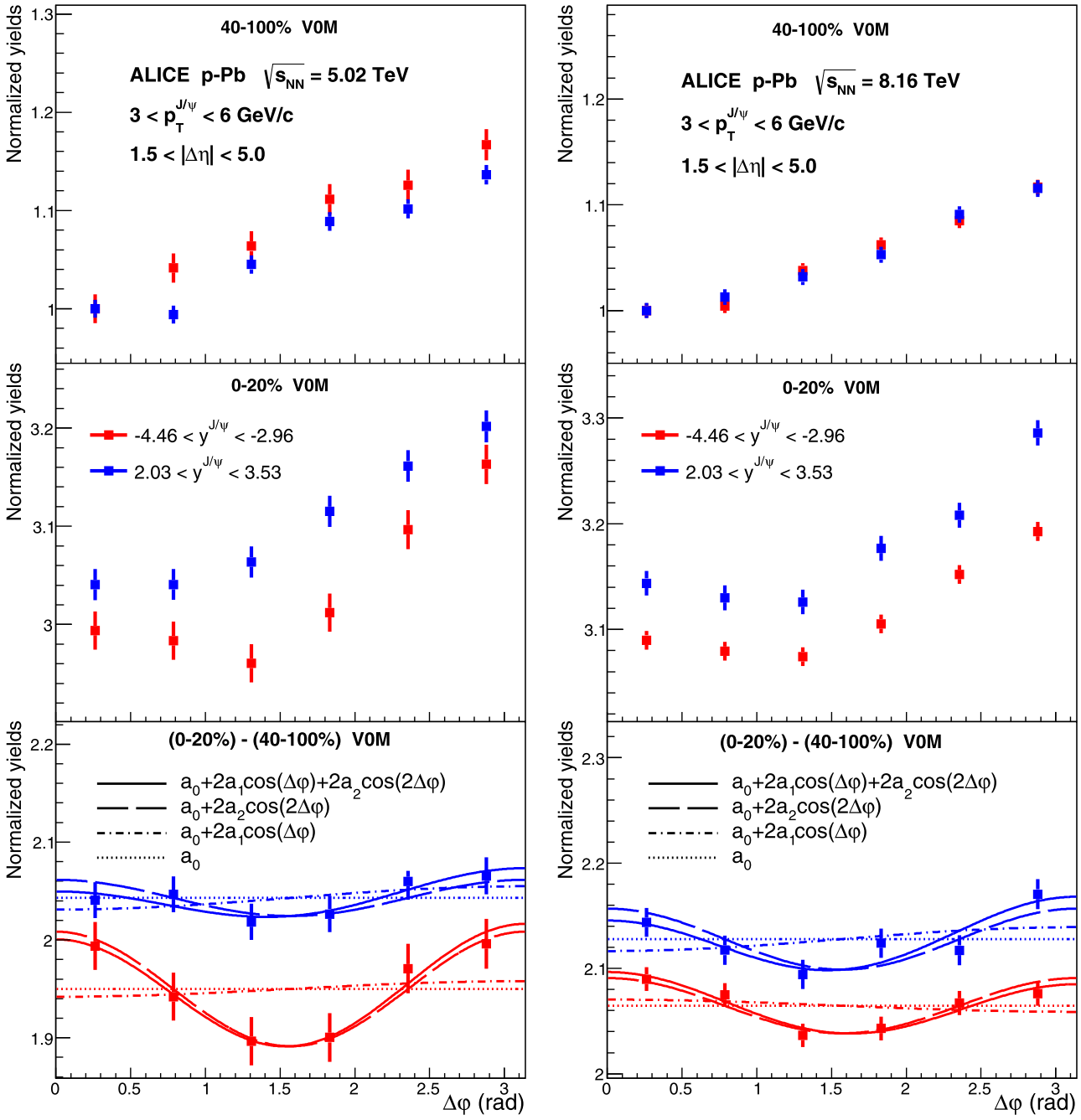

Fig. 3. Associated tracklet yields per J/ψ trigger in $3 < p_T^{J/\psi} < 6$ GeV/c in p–Pb and Pb–p collisions at $\sqrt{s_{NN}} = 5.02$ TeV (left panels) and 8.16 TeV (right panels). The top and the middle panels correspond to the low-multiplicity and the high-multiplicity event classes, respectively. The bottom panels show the yields after the subtraction of the low-multiplicity collision yields from the high-multiplicity collision ones. The solid line represent the fit to the data as described in the text. The dashed, dot-dashed and dotted lines correspond to the individual terms of the fit function defined in Eq. (3). All the yields are normalized to the value in $\Delta\varphi < \pi/6$ in the low-multiplicity (40–100%) event class. Only the statistical uncertainties are shown. (For interpretation of the colors in the figure(s), the reader is referred to the web version of this article.)

by employing various invariant mass fit functions, both for the background and for the J/ψ signal. The maximal difference of the results obtained with the above checks with respect to the default approach is taken as the corresponding systematic uncertainty.

The uncertainty arising from the employed analysis approach is obtained as the difference between the two extraction methods described in Section 4.

As described in Section 4, by default the mixed-event distribution $ME(\Delta\varphi, \Delta\eta)$ is normalized to unity in the $\Delta\eta$ region corresponding to the maximal acceptance. As an alternative approach, normalizing the integral of $ME(\Delta\varphi, \Delta\eta)$ to unity is used. No significant effect on the obtained results is observed and thus no systematic uncertainty is assigned.

The used event-mixing technique can introduce systematic biases. The event multiplicity distribution of the selected dimuons ($1 < M_{\mu\mu} < 5$ GeV/c^2) differs from that of the J/ψ signal. Since the charged-hadron spectra and the charged-hadron density as a function of η change with event multiplicity [34], the non-uniform (both in the azimuthal and longitudinal directions) SPD acceptance can introduce a bias. The corresponding systematic uncertainty is evaluated by doing the event mixing in finer event-multiplicity bins.

Table 1
Summary of absolute systematic uncertainties of the $v_2^{J/\psi}\{2, \text{sub}\}$ coefficients. The uncertainties vary within the indicated ranges depending on $p_T^{J/\psi}$. The values not preceded by a sign represent double-sided uncertainties.

Source of systematics	$\sqrt{s_{NN}} = 5.02$ TeV		$\sqrt{s_{NN}} = 8.16$ TeV	
	p–Pb	Pb–p	p–Pb	Pb–p
Acceptance correction	0 to 0.019	0 to 0.057	0 to 0.011	0 to 0.007
Background shape	0.007 to 0.013	0.015 to 0.056	0.011 to 0.013	0.003 to 0.012
Extraction method	0.003 to 0.015	0.010 to 0.040	0.002 to 0.011	0.008 to 0.018
Event mixing	0.003 to 0.015	0.004 to 0.025	0.002 to 0.008	0.004 to 0.012
Residual away-side jet correlation	–	−0.030 to 0	−0.018 to 0	–
Total	+0.009 to +0.024 −0.009 to −0.024	+0.024 to +0.084 −0.024 to −0.090	+0.013 to +0.019 −0.015 to −0.026	+0.015 to +0.021 −0.015 to −0.021

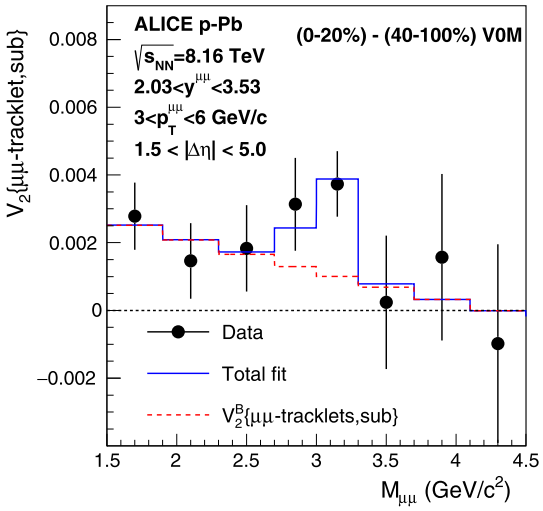

Fig. 4. Example of the fit from Eq. (4) in the $3 < p_T^{\mu\mu} < 6$ GeV/c interval for p–Pb collisions at $\sqrt{s_{NN}} = 8.16$ TeV. The dashed line corresponds to the $V_2^B\{\mu\mu - \text{tracklet, sub}\}(M_{\mu\mu})$.

The non-uniform acceptance of the muon spectrometer coupled to sizeable correlations between the dimuons and SPD tracklets can bias azimuthally the sample of SPD tracklets used for event mixing. In order to check for possible effects on our measurement, the event mixing is performed in intervals of azimuthal angle of the selected dimuons. We observe no significant systematic effect as the obtained results show negligible deviations with respect to the results using the default event-mixing technique.

The effect of a possible residual near-side peak is checked by varying the rapidity gap between the trigger dimuons and associated charged-hadrons from 1.0 to 2.0 units. We observe no indication of increasing v_2 with reduced gap and thus consider the default gap of 1.5 units sufficient to eliminate any significant residual near-side peak contribution.

As shown in Section 4, the recoil-jet away-side correlation structure in the high-multiplicity event class is greatly diminished after the subtraction of the low-multiplicity event class. By default, any remaining away-side structure is supposed to be taken into account by the $\cos\Delta\varphi$ term in Eq. (3). In order to check for residual effects we proceed in the following way. First, the correlation function in the low-multiplicity event class is fit with a Gaussian function centered at $\Delta\varphi = \pi$. Then, the correlation function in the high-multiplicity event class is fit with the function from Eq. (3), where the $\cos\Delta\varphi$ term is replaced by a Gaussian function with a width fixed to the value obtained from the fit in the low-multiplicity collisions. No clear signature of systematic change of the results is seen, except some hints of a possible effect in the highest $p_T^{J/\psi}$ interval. Conservatively, we assign systematic uncertainty as the difference with respect to the default analysis approach. Since the typical values of the Gaussian width are around 1 rad, one-sided (negative) systematic uncertainty is assigned.

In Table 1 we present a summary of the assigned systematic uncertainties of the $v_2^{J/\psi}\{2, \text{sub}\}$ coefficients. No sizeable correlations between the $p_T^{J/\psi}$ intervals are observed and therefore in the following the uncertainties are considered uncorrelated.

Our measurement is for inclusive J/ψ. The fraction of J/ψ from decays of b-hadrons reaches up to about 15% at $p_T^{J/\psi} \approx 6$ GeV/c in p–Pb collisions at $\sqrt{s_{NN}} = 5.02$ [40] and 8.16 TeV [41]. Therefore the feed-down contribution is unlikely to influence significantly our results. In principle, a possible strong multiplicity dependence of the feed-down fraction can potentially affect the subtraction approach. However, no evidence for such a strong dependence is observed in pp collisions [42].

As additional cross-checks the analysis is done using alternative event-multiplicity estimators, varying the tracklet $|\Delta\Phi|$ cut, applying a cut on the asymmetry of transverse momentum of the two muon tracks, removing the pile-up cuts and excluding the SPD regions with non-uniform acceptance in pseudorapidity. The corresponding results are found to be compatible with those obtained with the default analysis approach and therefore no further systematic uncertainties are assigned.

6. Results

In Fig. 5 we report the measured $v_2^{J/\psi}\{2, \text{sub}\}$ coefficients as a function of $p_T^{J/\psi}$ for p–Pb and Pb–p collisions at $\sqrt{s_{NN}} = 5.02$ and 8.16 TeV. Up to $p_T^{J/\psi}$ of 3 GeV/c, no significant deviation from zero is observed for either p–Pb or Pb–p collisions at the two collision energies. On the contrary, in the $p_T^{J/\psi}$ interval between 3 and 6 GeV/c, the $v_2^{J/\psi}\{2, \text{sub}\}$ is found to be positive although with large uncertainties. As also shown in Fig. 5, the $v_2^{J/\psi}$ coefficients in $2.5 < y < 4$ in central Pb–Pb collisions at $\sqrt{s_{NN}} = 5.02$ TeV reach maximal values in the same $p_T^{J/\psi}$ interval [24].

Two methods are employed in order to obtain the probability that the $v_2^{J/\psi}\{2, \text{sub}\}$ is zero in the $3 < p_T^{J/\psi} < 6$ GeV/c interval. In the first method, the $v_2^{J/\psi}\{2, \text{sub}\}$ values in the two $p_T^{J/\psi}$ intervals ($3 < p_T^{J/\psi} < 4$ GeV/c and $4 < p_T^{J/\psi} < 6$ GeV/c) are combined into a weighted average for each rapidity and collision energy. The obtained probabilities are 0.13% and 0.13% (7.8% and 0.23%) for p–Pb and Pb–p collisions, respectively, at $\sqrt{s_{NN}} = 8.16$ TeV (5.02 TeV). Combining all eight $v_2^{J/\psi}\{2, \text{sub}\}$ values yields a total probability of 1.7×10^{-7}. This corresponds to a 5.1σ significance of the measured positive $v_2^{J/\psi}\{2, \text{sub}\}$ coefficient. The second method is Fisher's combined probability test [43]. With this method one obtains probabilities of 0.14% and 0.23% (10.3% and 0.41%) for p–Pb and Pb–p collisions at $\sqrt{s_{NN}} = 8.16$ TeV (5.02 TeV), respectively.

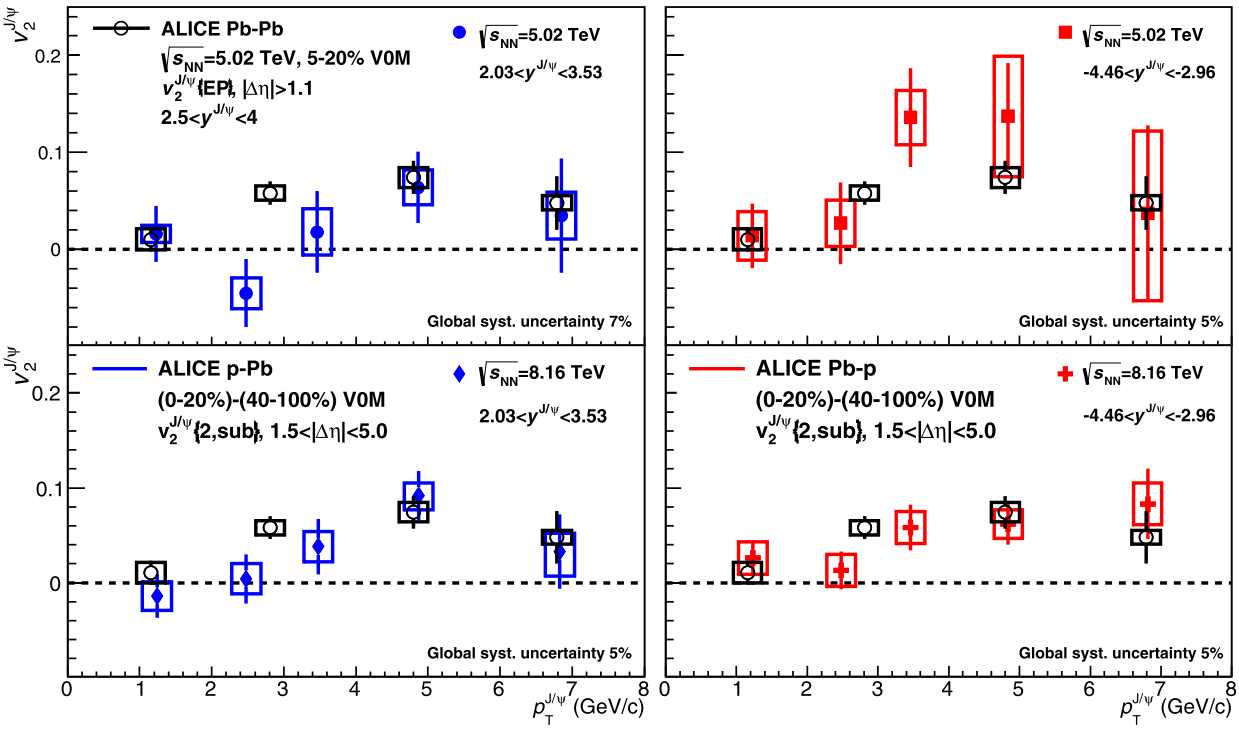

Fig. 5. $v_2^{\mathrm{J}/\psi}\{2,\mathrm{sub}\}$ in bins of $p_{\mathrm{T}}^{\mathrm{J}/\psi}$ for p–Pb, $2.03 < y < 3.53$ (left panels), and Pb–p, $-4.46 < y < -2.96$ (right panels), collisions at $\sqrt{s_{\mathrm{NN}}} = 5.02$ TeV (top panels) and 8.16 TeV (bottom panels). The results are compared to the $v_2^{\mathrm{J}/\psi}\{\mathrm{EP}\}$ coefficients measured in central Pb–Pb collisions at $\sqrt{s_{\mathrm{NN}}} = 5.02$ TeV in forward rapidity ($2.5 < y < 4$) using event plane (EP) based methods [24]. The statistical and uncorrelated systematic uncertainties are represented by lines and boxes, respectively. The quoted global systematic uncertainties correspond to the combined statistical and systematic uncertainties of the measured $v_2^{\mathrm{tracklet}}\{2,\mathrm{sub}\}$ coefficient.

The total probability is 1.4×10^{-6} which corresponds to a 4.7σ significance. In the calculation of the above probabilities, both statistical and systematic uncertainties of the measured values are taken into account. The global systematic uncertainty is not taken into account as it is irrelevant in the case of the zero hypothesis.

The analysis method presented in this Letter relies on the assumption that there are no significant correlations due to collective effects in the low-multiplicity event class. In case of a presence of such correlations, the measured $V_2\{\mathrm{J}/\psi - \mathrm{tracklet, sub}\}$ is equal to

$$V_2\{\mathrm{J}/\psi - \mathrm{tracklet, high}\} - \frac{b_0^{\mathrm{low}}}{b_0^{\mathrm{high}}} V_2\{\mathrm{J}/\psi - \mathrm{tracklet, low}\}, \qquad (6)$$

where $V_2\{\mathrm{J}/\psi - \mathrm{tracklet, high}\}$ and $V_2\{\mathrm{J}/\psi - \mathrm{tracklet, low}\}$ are the second-order Fourier coefficients of the azimuthal correlation between the J/ψ and the associated charged hadrons in the high-multiplicity and the low-multiplicity collisions, respectively, and $b_0^{\mathrm{low}}/b_0^{\mathrm{high}} \approx 1/3$ is the ratio of the combinatorial baseline in the low-multiplicity and high-multiplicity collisions (see Fig. 3). As is demonstrated in Ref. [44], the assumption of no significant collective correlations in the low-multiplicity collisions is certainly questionable for light-flavor hadrons. Our data indicates the same, as we observe a statistically significant increase of the measured values of $v_2^{\mathrm{tracklet}}\{2,\mathrm{sub}\}$ when subtracting a lower event-multiplicity, e.g. 60–100%, class. Ultimately, the value of the v_2^{tracklet} coefficient is found to be about 17% higher in case no subtraction is applied. Therefore, replacing the subtracted $v_2^{\mathrm{tracklet}}\{2,\mathrm{sub}\}$ coefficient in Eq. (5) by the non-subtracted coefficient would mean that the $v_2^{\mathrm{J}/\psi}$ coefficients are up to 17% lower with respect to the measured $v_2^{\mathrm{J}/\psi}\{2,\mathrm{sub}\}$ coefficients. However, assuming that the $v_2^{\mathrm{J}/\psi}$ coefficients follow the same trend as a function of event multiplicity as the v_2^{tracklet} coefficient, they would be up to 17% higher with respect to the measured $v_2^{\mathrm{J}/\psi}\{2,\mathrm{sub}\}$ coefficients. Subtracting lower event-multiplicity classes in the measurement of the $v_2^{\mathrm{J}/\psi}\{2,\mathrm{sub}\}$ coefficient does not improve the precision of our measurement, because of the limited amount of J/ψ signal in the low-multiplicity collisions.

The nuclear modification factor of J/ψ in p–Pb and Pb–p collisions [37,38] as well as the charged-particle v_2 coefficient [45–47] in pp collisions show no significant $\sqrt{s_{\mathrm{NN}}}$ dependence. As seen in Fig. 5, the measured $v_2^{\mathrm{J}/\psi}\{2,\mathrm{sub}\}$ coefficients at $\sqrt{s_{\mathrm{NN}}} = 5.02$ and 8.16 TeV also appear to be consistent with each other. The largest absolute difference between the results at the two collision energies is observed in Pb–p collisions in the $3 < p_{\mathrm{T}}^{\mathrm{J}/\psi} < 6$ GeV/c interval. The significance of this difference is rather low (below 1.5σ), because of the large uncertainties of the measurement at $\sqrt{s_{\mathrm{NN}}} = 5.02$ TeV. Hence, the data for the two collision energies are combined as a weighted average taking into account both statistical and systematic uncertainties. In Fig. 6, we present these combined results for p–Pb and Pb–p collisions together with measurements and model calculations for Pb–Pb collisions at $\sqrt{s_{\mathrm{NN}}} =$ 5.02 TeV [25].

In Pb–Pb collisions, the positive $v_2^{\mathrm{J}/\psi}$ coefficients at $p_{\mathrm{T}}^{\mathrm{J}/\psi}$ below 3–4 GeV/c are believed to originate from the recombination of charm quarks thermalized in the medium and are described fairly well by the transport model [25] (see Fig. 6). In p–Pb collisions, the amount of produced charm quarks is small and therefore the contribution from recombination should be negligible. Our measured values at $p_{\mathrm{T}}^{\mathrm{J}/\psi} < 3$ GeV/c are compatible with zero, in line with this expectation. There is one publication [28] which suggests that even in p–Pb collisions a sizeable contribution from recombination could occur due to canonical enhancement effects. The uncertainties of our results do not allow to confirm or to rule out this scenario.

In Pb–Pb collisions, the measured $v_2^{\mathrm{J}/\psi}$ coefficients exceed substantially the theoretical predictions at $p_{\mathrm{T}}^{\mathrm{J}/\psi} > 4$ GeV/c, where the

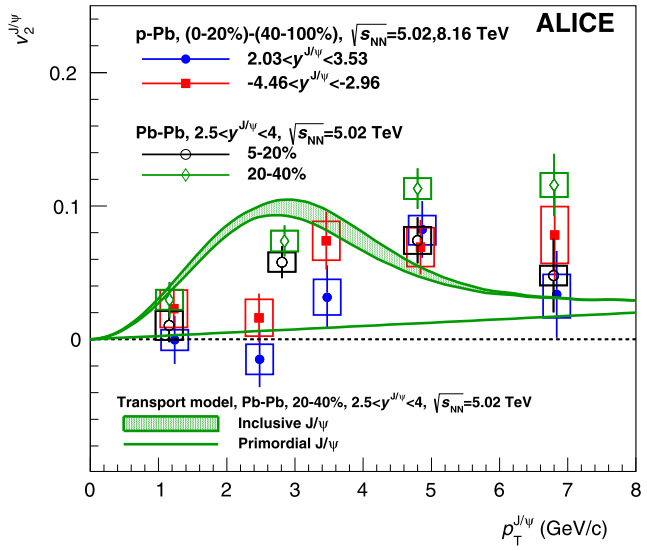

Fig. 6. Combined $v_2^{J/\psi}\{2, \text{sub}\}$ coefficients in p–Pb and Pb–p collisions compared to the results in central and semi-central Pb–Pb collisions at $\sqrt{s_{NN}} = 5.02$ TeV [24] and the transport model calculations for semi-central Pb–Pb collisions at $\sqrt{s_{NN}} = 5.02$ TeV [25]. The solid line corresponds to the contribution from path-length dependent suppression inside the medium. The band shows the resulting $v_2^{J/\psi}$ including also the recombination of thermalized charm quarks and the feed-down from b-hadron decays assuming thermalization of b quarks.

main contribution to $v_2^{J/\psi}$ is expected to come from path-length dependent suppression inside the medium [25] (see Fig. 6). In p–Pb collisions, the medium, if any, has a much smaller size [48] and hence very little, if any, path-length dependent effects are expected. In principle, the feed-down from decays of b-hadrons can give a positive $v_2^{J/\psi}$ at high transverse momentum in case of a positive b quark v_2. However, the latter would have to reach unreasonably high values given the magnitude of the measured $v_2^{J/\psi}\{2, \text{sub}\}$ and the small feed-down fraction. Despite these considerations, the measured positive $v_2^{J/\psi}$ coefficients would imply that the J/ψ participates in the collective behavior of the p–Pb collision system.

7. Summary

We presented a measurement of the angular correlations between forward and backward J/ψ and mid-rapidity charged hadrons in p–Pb and Pb–p collisions at $\sqrt{s_{NN}} = 5.02$ and 8.16 TeV. The data indicate persisting long-range correlation structures at $\Delta\varphi \approx 0$ and $\Delta\varphi \approx \pi$, reminiscent of the double ridge previously found in charged-particle correlations at mid- and forward rapidity. The corresponding $v_2^{J/\psi}\{2, \text{sub}\}$ coefficients in $3 < p_T^{J/\psi} < 6$ GeV/c are found to be positive with a total significance of 4.7σ to 5.1σ. The obtained values, albeit with large uncertainties, are comparable with those measured in Pb–Pb collisions at $\sqrt{s_{NN}} = 5.02$ TeV in forward rapidity. Although the underlying mechanism is not understood, the comparable magnitude of the $v_2^{J/\psi}$ coefficients at high transverse momentum in p–Pb and Pb–Pb collisions indicates that this mechanism could be similar in both collision systems.

Acknowledgements

The ALICE Collaboration would like to thank all its engineers and technicians for their invaluable contributions to the construction of the experiment and the CERN accelerator teams for the outstanding performance of the LHC complex. The ALICE Collaboration gratefully acknowledges the resources and support provided by all Grid centres and the Worldwide LHC Computing Grid (WLCG) collaboration. The ALICE Collaboration acknowledges the following funding agencies for their support in building and running the ALICE detector: A.I. Alikhanyan National Science Laboratory (Yerevan Physics Institute) Foundation (ANSL), State Committee of Science and World Federation of Scientists (WFS), Armenia; Austrian Academy of Sciences and Nationalstiftung für Forschung, Technologie und Entwicklung, Austria; Ministry of Communications and High Technologies, National Nuclear Research Center, Azerbaijan; Conselho Nacional de Desenvolvimento Científico e Tecnológico (CNPq), Universidade Federal do Rio Grande do Sul (UFRGS), Financiadora de Estudos e Projetos (Finep) and Fundação de Amparo à Pesquisa do Estado de São Paulo (FAPESP), Brazil; Ministry of Science & Technology of China (MSTC), National Natural Science Foundation of China (NSFC) and Ministry of Education of China (MOEC), China; Ministry of Science, Education and Sports and Croatian Science Foundation, Croatia; Ministry of Education, Youth and Sports of the Czech Republic, Czech Republic; The Danish Council for Independent Research – Natural Sciences, the Carlsberg Foundation and Danish National Research Foundation (DNRF), Denmark; Helsinki Institute of Physics (HIP), Finland; Commissariat à l'Energie Atomique (CEA) and Institut National de Physique Nucléaire et de Physique des Particules (IN2P3) and Centre National de la Recherche Scientifique (CNRS), France; Bundesministerium für Bildung, Wissenschaft, Forschung und Technologie (BMBF) and GSI Helmholtzzentrum für Schwerionenforschung GmbH, Germany; General Secretariat for Research and Technology, Ministry of Education, Research and Religions, Greece; National Research, Development and Innovation Office, Hungary; Department of Atomic Energy, Government of India (DAE), Department of Science and Technology, Government of India (DST), University Grants Commission, Government of India (UGC) and Council of Scientific and Industrial Research (CSIR), India; Indonesian Institute of Science, Indonesia; Centro Fermi – Museo Storico della Fisica e Centro Studi e Ricerche Enrico Fermi and Istituto Nazionale di Fisica Nucleare (INFN), Italy; Institute for Innovative Science and Technology, Nagasaki Institute of Applied Science (IIST), Japan Society for the Promotion of Science (JSPS) KAKENHI and Japanese Ministry of Education, Culture, Sports, Science and Technology (MEXT), Japan; Consejo Nacional de Ciencia (CONACYT) y Tecnología, through Fondo de Cooperación Internacional en Ciencia y Tecnología (FONCICYT) and Dirección General de Asuntos del Personal Academico (DGAPA), Mexico; Nederlandse Organisatie voor Wetenschappelijk Onderzoek (NWO), Netherlands; The Research Council of Norway, Norway; Commission on Science and Technology for Sustainable Development in the South (COMSATS), Pakistan; Pontificia Universidad Católica del Perú, Peru; Ministry of Science and Higher Education and National Science Centre, Poland; Korea Institute of Science and Technology Information and National Research Foundation of Korea (NRF), Republic of Korea; Ministry of Education and Scientific Research, Institute of Atomic Physics and Romanian National Agency for Science, Technology and Innovation, Romania; Joint Institute for Nuclear Research (JINR), Ministry of Education and Science of the Russian Federation and National Research Centre Kurchatov Institute, Russia; Ministry of Education, Science, Research and Sport of the Slovak Republic, Slovakia; National Research Foundation of South Africa, South Africa; Centro de Aplicaciones Tecnológicas y Desarrollo Nuclear (CEADEN), Cubaenergía, Cuba, Ministerio de Ciencia e Innovacion and Centro de Investigaciones Energéticas, Medioambientales y Tecnológicas (CIEMAT), Spain; Swedish Research Council (VR) and Knut & Alice Wallenberg Foundation (KAW), Sweden; European Organization for Nuclear Research, Switzerland; National Science and Technology Development Agency (NSDTA), Suranaree University of Technol-

ogy (SUT) and Office of the Higher Education Commission under NRU project of Thailand, Thailand; Turkish Atomic Energy Agency (TAEK), Turkey; National Academy of Sciences of Ukraine, Ukraine; Science and Technology Facilities Council (STFC), United Kingdom; National Science Foundation of the United States of America (NSF) and United States Department of Energy, Office of Nuclear Physics (DOE NP), United States of America.

References

[1] X.-N. Wang, Studying mini-jets via the p_T dependence of the two particle correlation in azimuthal angle Phi, Phys. Rev. D 47 (1993) 2754–2760, arXiv:hep-ph/9306215.
[2] ALICE Collaboration, K. Aamodt, et al., Harmonic decomposition of two-particle angular correlations in Pb–Pb collisions at $\sqrt{s_{NN}} = 2.76$ TeV, Phys. Lett. B 708 (2012) 249–264, arXiv:1109.2501 [nucl-ex].
[3] CMS Collaboration, V. Khachatryan, et al., Observation of long-range near-side angular correlations in proton–proton collisions at the LHC, J. High Energy Phys. 09 (2010) 091, arXiv:1009.4122 [hep-ex].
[4] CMS Collaboration, S. Chatrchyan, et al., Observation of long-range near-side angular correlations in proton–lead collisions at the LHC, Phys. Lett. B 718 (2013) 795–814, arXiv:1210.5482 [nucl-ex].
[5] ALICE Collaboration, B. Abelev, et al., Long-range angular correlations on the near and away side in p–Pb collisions at $\sqrt{s_{NN}} = 5.02$ TeV, Phys. Lett. B 719 (2013) 29–41, arXiv:1212.2001 [nucl-ex].
[6] ATLAS Collaboration, G. Aad, et al., Observation of associated near-side and away-side long-range correlations in $\sqrt{s_{NN}} = 5.02$ TeV proton–lead collisions with the ATLAS detector, Phys. Rev. Lett. 110 (18) (2013) 182302, arXiv:1212.5198 [hep-ex].
[7] PHENIX Collaboration, A. Adare, et al., Quadrupole anisotropy in dihadron azimuthal correlations in central d+Au collisions at $\sqrt{s_{NN}} = 200$ GeV, Phys. Rev. Lett. 111 (21) (2013) 212301, arXiv:1303.1794 [nucl-ex].
[8] STAR Collaboration, L. Adamczyk, et al., Long-range pseudorapidity dihadron correlations in d+Au collisions at $\sqrt{s_{\rm NN}} = 200$ GeV, Phys. Lett. B 747 (2015) 265–271, arXiv:1502.07652 [nucl-ex].
[9] CMS Collaboration, V. Khachatryan, et al., Evidence for collective multiparticle correlations in p–Pb collisions, Phys. Rev. Lett. 115 (1) (2015) 012301, arXiv:1502.05382 [nucl-ex].
[10] ALICE Collaboration, B.B. Abelev, et al., Multiparticle azimuthal correlations in p–Pb and Pb–Pb collisions at the CERN Large Hadron Collider, Phys. Rev. C 90 (5) (2014) 054901, arXiv:1406.2474 [nucl-ex].
[11] ATLAS Collaboration, M. Aaboud, et al., Measurement of multi-particle azimuthal correlations in pp, p+Pb and low-multiplicity Pb+Pb collisions with the ATLAS detector, Eur. Phys. J. C 77 (6) (2017) 428, arXiv:1705.04176 [hep-ex].
[12] ALICE Collaboration, B.B. Abelev, et al., Long-range angular correlations of π, K and p in p–Pb collisions at $\sqrt{s_{\rm NN}} = 5.02$ TeV, Phys. Lett. B 726 (2013) 164–177, arXiv:1307.3237 [nucl-ex].
[13] CMS Collaboration, V. Khachatryan, et al., Long-range two-particle correlations of strange hadrons with charged particles in pPb and PbPb collisions at LHC energies, Phys. Lett. B 742 (2015) 200–224, arXiv:1409.3392 [nucl-ex].
[14] K. Dusling, R. Venugopalan, Comparison of the color glass condensate to dihadron correlations in proton–proton and proton–nucleus collisions, Phys. Rev. D 87 (9) (2013) 094034, arXiv:1302.7018 [hep-ph].
[15] A. Bzdak, G.-L. Ma, Elliptic and triangular flow in p+Pb and peripheral Pb+Pb collisions from parton scatterings, Phys. Rev. Lett. 113 (25) (2014) 252301, arXiv:1406.2804 [hep-ph].
[16] ALICE Collaboration, J. Adam, et al., Forward-central two-particle correlations in p–Pb collisions at $\sqrt{s_{\rm NN}} = 5.02$ TeV, Phys. Lett. B 753 (2016) 126–139, arXiv:1506.08032 [nucl-ex].
[17] A. Andronic, et al., Heavy-flavour and quarkonium production in the LHC era: from proton–proton to heavy-ion collisions, Eur. Phys. J. C 76 (3) (2016) 107, arXiv:1506.03981 [nucl-ex].
[18] K.J. Eskola, H. Paukkunen, C.A. Salgado, EPS09: a new generation of NLO and LO nuclear parton distribution functions, J. High Energy Phys. 04 (2009) 065, arXiv:0902.4154 [hep-ph].
[19] J.-w. Qiu, J.P. Vary, X.-f. Zhang, J/ψ suppression in nucleus–nucleus collisions, Phys. Rev. Lett. 88 (2002) 232301, arXiv:hep-ph/9809442.
[20] F. Arleo, S. Peigne, Heavy-quarkonium suppression in p–A collisions from parton energy loss in cold QCD matter, J. High Energy Phys. 03 (2013) 122, arXiv:1212.0434 [hep-ph].
[21] T. Matsui, H. Satz, J/ψ suppression by quark–gluon plasma formation, Phys. Lett. B 178 (1986) 416–422.
[22] R.L. Thews, M. Schroedter, J. Rafelski, Enhanced J/ψ production in deconfined quark matter, Phys. Rev. C 63 (2001) 054905, arXiv:hep-ph/0007323.
[23] P. Braun-Munzinger, J. Stachel, (Non)thermal aspects of charmonium production and a new look at J/ψ suppression, Phys. Lett. B 490 (2000) 196–202, arXiv:nucl-th/0007059.
[24] ALICE Collaboration, S. Acharya, et al., J/ψ elliptic flow in Pb–Pb collisions at $\sqrt{s_{\rm NN}} = 5.02$ TeV, arXiv:1709.05260 [nucl-ex].
[25] X. Du, R. Rapp, Sequential regeneration of charmonia in heavy-ion collisions, Nucl. Phys. A 943 (2015) 147–158, arXiv:1504.00670 [hep-ph].
[26] X. Zhao, A. Emerick, R. Rapp, In-medium quarkonia at SPS, RHIC and LHC, Nucl. Phys. A 904–905 (2013) 611c–614c, arXiv:1210.6583 [hep-ph].
[27] B. Chen, T. Guo, Y. Liu, P. Zhuang, Cold and hot nuclear matter effects on charmonium production in p+Pb collisions at LHC energy, Phys. Lett. B 765 (2017) 323–327, arXiv:1607.07927 [nucl-th].
[28] Y. Liu, C.M. Ko, T. Song, Hot medium effects on J/ψ production in p+Pb collisions at $\sqrt{s_{NN}} = 5.02$ TeV, Phys. Lett. B 728 (2014) 437–442, arXiv:1309.5113 [nucl-th].
[29] E.G. Ferreiro, Excited charmonium suppression in proton–nucleus collisions as a consequence of comovers, Phys. Lett. B 749 (2015) 98–103, arXiv:1411.0549 [hep-ph].
[30] ALICE Collaboration, K. Aamodt, et al., The ALICE experiment at the CERN LHC, J. Instrum. 3 (2008) S08002.
[31] ALICE Collaboration, K. Aamodt, et al., Alignment of the ALICE Inner Tracking System with cosmic-ray tracks, J. Instrum. 5 (2010) P03003, arXiv:1001.0502 [physics.ins-det].
[32] ALICE Collaboration, J. Adam, et al., Charged-particle multiplicities in proton–proton collisions at $\sqrt{s} = 0.9$ to 8 TeV, Eur. Phys. J. C 77 (1) (2017) 33, arXiv:1509.07541 [nucl-ex].
[33] ALICE Collaboration, E. Abbas, et al., Performance of the ALICE VZERO system, J. Instrum. 8 (2013) P10016, arXiv:1306.3130 [nucl-ex].
[34] ALICE Collaboration, J. Adam, et al., Centrality dependence of particle production in p–Pb collisions at $\sqrt{s_{\rm NN}} = 5.02$ TeV, Phys. Rev. C 91 (6) (2015) 064905, arXiv:1412.6828 [nucl-ex].
[35] ALICE Collaboration, B. Abelev, et al., Heavy flavour decay muon production at forward rapidity in proton–proton collisions at $\sqrt{s} = 7$ TeV, Phys. Lett. B 708 (2012) 265–275, arXiv:1201.3791 [hep-ex].
[36] ALICE Collaboration, Quarkonium signal extraction in ALICE, https://cds.cern.ch/record/2060096. ALICE-PUBLIC-2015-006.
[37] ALICE Collaboration, B.B. Abelev, et al., J/ψ production and nuclear effects in p–Pb collisions at $\sqrt{s_{\rm NN}} = 5.02$ TeV, J. High Energy Phys. 02 (2014) 073, arXiv:1308.6726 [nucl-ex].
[38] ALICE Collaboration, Preliminary physics summary: inclusive J/ψ production at forward rapidity in p–Pb collisions at $\sqrt{s_{\rm NN}} = 8.16$ TeV, https://cds.cern.ch/record/2244670. ALICE-PUBLIC-2017-001.
[39] R. Barlow, Systematic errors: facts and fictions, in: Advanced Statistical Techniques in Particle Physics. Proceedings, Conference, Durham, UK, March 18–22, 2002, 2002, pp. 134–144, arXiv:hep-ex/0207026.
[40] LHCb Collaboration, R. Aaij, et al., Study of J/ψ production and cold nuclear matter effects in pPb collisions at $\sqrt{s_{NN}} = 5$ TeV, J. High Energy Phys. 02 (2014) 072, arXiv:1308.6729 [nucl-ex].
[41] LHCb Collaboration, R. Aaij, et al., Prompt and nonprompt J/ψ production and nuclear modification in pPb collisions at $\sqrt{s_{\rm NN}} = 8.16$ TeV, arXiv:1706.07122 [hep-ex].
[42] ALICE Collaboration, J. Adam, et al., Measurement of charm and beauty production at central rapidity versus charged-particle multiplicity in proton–proton collisions at $\sqrt{s} = 7$ TeV, J. High Energy Phys. 09 (2015) 148, arXiv:1505.00664 [nucl-ex].
[43] R.A. Fisher, Statistical Methods for Research Workers, Springer New York, New York, NY, 1992, pp. 66–70, https://doi.org/10.1007/978-1-4612-4380-9_6.
[44] ATLAS Collaboration, M. Aaboud, et al., Measurements of long-range azimuthal anisotropies and associated Fourier coefficients for pp collisions at $\sqrt{s} = 5.02$ and 13 TeV and p+Pb collisions at $\sqrt{s_{\rm NN}} = 5.02$ TeV with the ATLAS detector, arXiv:1609.06213 [nucl-ex].
[45] ATLAS Collaboration, G. Aad, et al., Observation of long-range elliptic azimuthal anisotropies in $\sqrt{s} = 13$ and 2.76 TeV pp collisions with the ATLAS detector, Phys. Rev. Lett. 116 (17) (2016) 172301, arXiv:1509.04776 [hep-ex].
[46] CMS Collaboration, V. Khachatryan, et al., Measurement of long-range near-side two-particle angular correlations in pp collisions at $\sqrt{s} = 13$ TeV, Phys. Rev. Lett. 116 (17) (2016) 172302, arXiv:1510.03068 [nucl-ex].
[47] CMS Collaboration, V. Khachatryan, et al., Evidence for collectivity in pp collisions at the LHC, Phys. Lett. B 765 (2017) 193–220, arXiv:1606.06198 [nucl-ex].
[48] ALICE Collaboration, J. Adam, et al., Two-pion femtoscopy in p–Pb collisions at $\sqrt{s_{\rm NN}} = 5.02$ TeV, Phys. Rev. C 91 (2015) 034906, arXiv:1502.00559 [nucl-ex].

ALICE Collaboration

S. Acharya [137], D. Adamová [94], J. Adolfsson [34], M.M. Aggarwal [99], G. Aglieri Rinella [35], M. Agnello [31], N. Agrawal [48], Z. Ahammed [137], S.U. Ahn [79], S. Aiola [141], A. Akindinov [64], M. Al-Turany [106], S.N. Alam [137], D.S.D. Albuquerque [122], D. Aleksandrov [90], B. Alessandro [58], R. Alfaro Molina [74], Y. Ali [15], A. Alici [12,53,27], A. Alkin [3], J. Alme [22], T. Alt [70], L. Altenkamper [22], I. Altsybeev [136], C. Alves Garcia Prado [121], C. Andrei [87], D. Andreou [35], H.A. Andrews [110], A. Andronic [106], V. Anguelov [104], C. Anson [97], T. Antičić [107], F. Antinori [56], P. Antonioli [53], L. Aphecetche [114], H. Appelshäuser [70], S. Arcelli [27], R. Arnaldi [58], O.W. Arnold [105,36], I.C. Arsene [21], M. Arslandok [104], B. Audurier [114], A. Augustinus [35], R. Averbeck [106], M.D. Azmi [17], A. Badalà [55], Y.W. Baek [60,78], S. Bagnasco [58], R. Bailhache [70], R. Bala [101], A. Baldisseri [75], M. Ball [45], R.C. Baral [67,88], A.M. Barbano [26], R. Barbera [28], F. Barile [33], L. Barioglio [26], G.G. Barnaföldi [140], L.S. Barnby [93], V. Barret [131], P. Bartalini [7], K. Barth [35], E. Bartsch [70], N. Bastid [131], S. Basu [139], G. Batigne [114], B. Batyunya [77], P.C. Batzing [21], J.L. Bazo Alba [111], I.G. Bearden [91], H. Beck [104], C. Bedda [63], N.K. Behera [60], I. Belikov [133], F. Bellini [27,35], H. Bello Martinez [2], R. Bellwied [124], L.G.E. Beltran [120], V. Belyaev [83], G. Bencedi [140], S. Beole [26], A. Bercuci [87], Y. Berdnikov [96], D. Berenyi [140], R.A. Bertens [127], D. Berzano [35], L. Betev [35], A. Bhasin [101], I.R. Bhat [101], B. Bhattacharjee [44], J. Bhom [118], A. Bianchi [26], L. Bianchi [124], N. Bianchi [51], C. Bianchin [139], J. Bielčík [39], J. Bielčíková [94], A. Bilandzic [36,105], G. Biro [140], R. Biswas [4], S. Biswas [4], J.T. Blair [119], D. Blau [90], C. Blume [70], G. Boca [134], F. Bock [35], A. Bogdanov [83], L. Boldizsár [140], M. Bombara [40], G. Bonomi [135], M. Bonora [35], J. Book [70], H. Borel [75], A. Borissov [104,19], M. Borri [126], E. Botta [26], C. Bourjau [91], L. Bratrud [70], P. Braun-Munzinger [106], M. Bregant [121], T.A. Broker [70], M. Broz [39], E.J. Brucken [46], E. Bruna [58], G.E. Bruno [35,33], D. Budnikov [108], H. Buesching [70], S. Bufalino [31], P. Buhler [113], P. Buncic [35], O. Busch [130], Z. Buthelezi [76], J.B. Butt [15], J.T. Buxton [18], J. Cabala [116], D. Caffarri [35,92], H. Caines [141], A. Caliva [63,106], E. Calvo Villar [111], P. Camerini [25], A.A. Capon [113], F. Carena [35], W. Carena [35], F. Carnesecchi [27,12], J. Castillo Castellanos [75], A.J. Castro [127], E.A.R. Casula [54], C. Ceballos Sanchez [9], S. Chandra [137], B. Chang [125], W. Chang [7], S. Chapeland [35], M. Chartier [126], S. Chattopadhyay [137], S. Chattopadhyay [109], A. Chauvin [36,105], C. Cheshkov [132], B. Cheynis [132], V. Chibante Barroso [35], D.D. Chinellato [122], S. Cho [60], P. Chochula [35], M. Chojnacki [91], S. Choudhury [137], T. Chowdhury [131], P. Christakoglou [92], C.H. Christensen [91], P. Christiansen [34], T. Chujo [130], S.U. Chung [19], C. Cicalo [54], L. Cifarelli [12,27], F. Cindolo [53], J. Cleymans [100], F. Colamaria [52,33], D. Colella [35,52,65], A. Collu [82], M. Colocci [27], M. Concas [58,ii], G. Conesa Balbastre [81], Z. Conesa del Valle [61], J.G. Contreras [39], T.M. Cormier [95], Y. Corrales Morales [58], I. Cortés Maldonado [2], P. Cortese [32], M.R. Cosentino [123], F. Costa [35], S. Costanza [134], J. Crkovská [61], P. Crochet [131], E. Cuautle [72], L. Cunqueiro [95,71], T. Dahms [36,105], A. Dainese [56], M.C. Danisch [104], A. Danu [68], D. Das [109], I. Das [109], S. Das [4], A. Dash [88], S. Dash [48], S. De [49], A. De Caro [30], G. de Cataldo [52], C. de Conti [121], J. de Cuveland [42], A. De Falco [24], D. De Gruttola [30,12], N. De Marco [58], S. De Pasquale [30], R.D. De Souza [122], H.F. Degenhardt [121], A. Deisting [106,104], A. Deloff [86], C. Deplano [92], P. Dhankher [48], D. Di Bari [33], A. Di Mauro [35], P. Di Nezza [51], B. Di Ruzza [56], M.A. Diaz Corchero [10], T. Dietel [100], P. Dillenseger [70], Y. Ding [7], R. Divià [35], Ø. Djuvsland [22], A. Dobrin [35], D. Domenicis Gimenez [121], B. Dönigus [70], O. Dordic [21], L.V.R. Doremalen [63], A.K. Dubey [137], A. Dubla [106], L. Ducroux [132], S. Dudi [99], A.K. Duggal [99], M. Dukhishyam [88], P. Dupieux [131], R.J. Ehlers [141], D. Elia [52], E. Endress [111], H. Engel [69], E. Epple [141], B. Erazmus [114], F. Erhardt [98], B. Espagnon [61], G. Eulisse [35], J. Eum [19], D. Evans [110], S. Evdokimov [112], L. Fabbietti [105,36], J. Faivre [81], A. Fantoni [51], M. Fasel [95], L. Feldkamp [71], A. Feliciello [58], G. Feofilov [136], A. Fernández Téllez [2], E.G. Ferreiro [16], A. Ferretti [26], A. Festanti [29,35], V.J.G. Feuillard [75,131], J. Figiel [118], M.A.S. Figueredo [121], S. Filchagin [108], D. Finogeev [62], F.M. Fionda [22,24], M. Floris [35], S. Foertsch [76], P. Foka [106], S. Fokin [90], E. Fragiacomo [59], A. Francescon [35], A. Francisco [114], U. Frankenfeld [106], G.G. Fronze [26], U. Fuchs [35], C. Furget [81], A. Furs [62], M. Fusco Girard [30], J.J. Gaardhøje [91], M. Gagliardi [26], A.M. Gago [111], K. Gajdosova [91], M. Gallio [26], C.D. Galvan [120], P. Ganoti [85], C. Garabatos [106], E. Garcia-Solis [13], K. Garg [28], C. Gargiulo [35], P. Gasik [105,36], E.F. Gauger [119], M.B. Gay Ducati [73], M. Germain [114], J. Ghosh [109], P. Ghosh [137], S.K. Ghosh [4], P. Gianotti [51], P. Giubellino [35,106,58], P. Giubilato [29], E. Gladysz-Dziadus [118], P. Glässel [104], D.M. Goméz Coral [74], A. Gomez Ramirez [69], A.S. Gonzalez [35], V. Gonzalez [10], P. González-Zamora [10,2], S. Gorbunov [42], L. Görlich [118], S. Gotovac [117], V. Grabski [74], L.K. Graczykowski [138], K.L. Graham [110], L. Greiner [82], A. Grelli [63], C. Grigoras [35], V. Grigoriev [83], A. Grigoryan [1], S. Grigoryan [77], J.M. Gronefeld [106], F. Grosa [31],

J.F. Grosse-Oetringhaus [35], R. Grosso [106], F. Guber [62], R. Guernane [81], B. Guerzoni [27], K. Gulbrandsen [91], T. Gunji [129], A. Gupta [101], R. Gupta [101], I.B. Guzman [2], R. Haake [35], C. Hadjidakis [61], H. Hamagaki [84], G. Hamar [140], J.C. Hamon [133], M.R. Haque [63], J.W. Harris [141], A. Harton [13], H. Hassan [81], D. Hatzifotiadou [12,53], S. Hayashi [129], S.T. Heckel [70], E. Hellbär [70], H. Helstrup [37], A. Herghelegiu [87], E.G. Hernandez [2], G. Herrera Corral [11], F. Herrmann [71], B.A. Hess [103], K.F. Hetland [37], H. Hillemanns [35], C. Hills [126], B. Hippolyte [133], B. Hohlweger [105], D. Horak [39], S. Hornung [106], R. Hosokawa [81,130], P. Hristov [35], C. Hughes [127], T.J. Humanic [18], N. Hussain [44], T. Hussain [17], D. Hutter [42], D.S. Hwang [20], S.A. Iga Buitron [72], R. Ilkaev [108], M. Inaba [130], M. Ippolitov [83,90], M.S. Islam [109], M. Ivanov [106], V. Ivanov [96], V. Izucheev [112], B. Jacak [82], N. Jacazio [27], P.M. Jacobs [82], M.B. Jadhav [48], S. Jadlovska [116], J. Jadlovsky [116], S. Jaelani [63], C. Jahnke [36], M.J. Jakubowska [138], M.A. Janik [138], P.H.S.Y. Jayarathna [124], C. Jena [88], M. Jercic [98], R.T. Jimenez Bustamante [106], P.G. Jones [110], A. Jusko [110], P. Kalinak [65], A. Kalweit [35], J.H. Kang [142], V. Kaplin [83], S. Kar [137], A. Karasu Uysal [80], O. Karavichev [62], T. Karavicheva [62], L. Karayan [106,104], P. Karczmarczyk [35], E. Karpechev [62], U. Kebschull [69], R. Keidel [143], D.L.D. Keijdener [63], M. Keil [35], B. Ketzer [45], Z. Khabanova [92], P. Khan [109], S.A. Khan [137], A. Khanzadeev [96], Y. Kharlov [112], A. Khatun [17], A. Khuntia [49], M.M. Kielbowicz [118], B. Kileng [37], B. Kim [130], D. Kim [142], D.J. Kim [125], H. Kim [142], J.S. Kim [43], J. Kim [104], M. Kim [60], S. Kim [20], T. Kim [142], S. Kirsch [42], I. Kisel [42], S. Kiselev [64], A. Kisiel [138], G. Kiss [140], J.L. Klay [6], C. Klein [70], J. Klein [35], C. Klein-Bösing [71], S. Klewin [104], A. Kluge [35], M.L. Knichel [104,35], A.G. Knospe [124], C. Kobdaj [115], M. Kofarago [140], M.K. Köhler [104], T. Kollegger [106], V. Kondratiev [136], N. Kondratyeva [83], E. Kondratyuk [112], A. Konevskikh [62], M. Konyushikhin [139], M. Kopcik [116], M. Kour [101], C. Kouzinopoulos [35], O. Kovalenko [86], V. Kovalenko [136], M. Kowalski [118], G. Koyithatta Meethaleveedu [48], I. Králik [65], A. Kravčáková [40], L. Kreis [106], M. Krivda [110,65], F. Krizek [94], E. Kryshen [96], M. Krzewicki [42], A.M. Kubera [18], V. Kučera [94], C. Kuhn [133], P.G. Kuijer [92], A. Kumar [101], J. Kumar [48], L. Kumar [99], S. Kumar [48], S. Kundu [88], P. Kurashvili [86], A. Kurepin [62], A.B. Kurepin [62], A. Kuryakin [108], S. Kushpil [94], M.J. Kweon [60], Y. Kwon [142], S.L. La Pointe [42], P. La Rocca [28], C. Lagana Fernandes [121], Y.S. Lai [82], I. Lakomov [35], R. Langoy [41], K. Lapidus [141], C. Lara [69], A. Lardeux [21], A. Lattuca [26], E. Laudi [35], R. Lavicka [39], R. Lea [25], L. Leardini [104], S. Lee [142], F. Lehas [92], S. Lehner [113], J. Lehrbach [42], R.C. Lemmon [93], E. Leogrande [63], I. León Monzón [120], P. Lévai [140], X. Li [14], J. Lien [41], R. Lietava [110], B. Lim [19], S. Lindal [21], V. Lindenstruth [42], S.W. Lindsay [126], C. Lippmann [106], M.A. Lisa [18], V. Litichevskyi [46], W.J. Llope [139], D.F. Lodato [63], P.I. Loenne [22], V. Loginov [83], C. Loizides [95,82], P. Loncar [117], X. Lopez [131], E. López Torres [9], A. Lowe [140], P. Luettig [70], J.R. Luhder [71], M. Lunardon [29], G. Luparello [59,25], M. Lupi [35], T.H. Lutz [141], A. Maevskaya [62], M. Mager [35], S.M. Mahmood [21], A. Maire [133], R.D. Majka [141], M. Malaev [96], L. Malinina [77,iii], D. Mal'Kevich [64], P. Malzacher [106], A. Mamonov [108], V. Manko [90], F. Manso [131], V. Manzari [52], Y. Mao [7], M. Marchisone [132,76,128], J. Mareš [66], G.V. Margagliotti [25], A. Margotti [53], J. Margutti [63], A. Marín [106], C. Markert [119], M. Marquard [70], N.A. Martin [106], P. Martinengo [35], J.A.L. Martinez [69], M.I. Martínez [2], G. Martínez García [114], M. Martinez Pedreira [35], S. Masciocchi [106], M. Masera [26], A. Masoni [54], E. Masson [114], A. Mastroserio [52], A.M. Mathis [105,36], P.F.T. Matuoka [121], A. Matyja [127], C. Mayer [118], J. Mazer [127], M. Mazzilli [33], M.A. Mazzoni [57], F. Meddi [23], Y. Melikyan [83], A. Menchaca-Rocha [74], E. Meninno [30], J. Mercado Pérez [104], M. Meres [38], S. Mhlanga [100], Y. Miake [130], M.M. Mieskolainen [46], D.L. Mihaylov [105], K. Mikhaylov [77,64], A. Mischke [63], A.N. Mishra [49], D. Miśkowiec [106], J. Mitra [137], C.M. Mitu [68], N. Mohammadi [63], A.P. Mohanty [63], B. Mohanty [88], M. Mohisin Khan [17,iv], E. Montes [10], D.A. Moreira De Godoy [71], L.A.P. Moreno [2], S. Moretto [29], A. Morreale [114], A. Morsch [35], V. Muccifora [51], E. Mudnic [117], D. Mühlheim [71], S. Muhuri [137], J.D. Mulligan [141], M.G. Munhoz [121], K. Münning [45], R.H. Munzer [70], H. Murakami [129], S. Murray [76], L. Musa [35], J. Musinsky [65], C.J. Myers [124], J.W. Myrcha [138], D. Nag [4], B. Naik [48], R. Nair [86], B.K. Nandi [48], R. Nania [12,53], E. Nappi [52], A. Narayan [48], M.U. Naru [15], H. Natal da Luz [121], C. Nattrass [127], S.R. Navarro [2], K. Nayak [88], R. Nayak [48], T.K. Nayak [137], S. Nazarenko [108], R.A. Negrao De Oliveira [70,35], L. Nellen [72], S.V. Nesbo [37], F. Ng [124], M. Nicassio [106], M. Niculescu [68], J. Niedziela [35,138], B.S. Nielsen [91], S. Nikolaev [90], S. Nikulin [90], V. Nikulin [96], F. Noferini [12,53], P. Nomokonov [77], G. Nooren [63], J.C.C. Noris [2], J. Norman [126], A. Nyanin [90], J. Nystrand [22], H. Oeschler [19,104,i], H. Oh [142], A. Ohlson [104], T. Okubo [47], L. Olah [140], J. Oleniacz [138], A.C. Oliveira Da Silva [121], M.H. Oliver [141], J. Onderwaater [106], C. Oppedisano [58], R. Orava [46], M. Oravec [116], A. Ortiz Velasquez [72], A. Oskarsson [34], J. Otwinowski [118], K. Oyama [84], Y. Pachmayer [104], V. Pacik [91], D. Pagano [135], G. Paić [72], P. Palni [7], J. Pan [139], A.K. Pandey [48], S. Panebianco [75], V. Papikyan [1],

P. Pareek [49], J. Park [60], S. Parmar [99], A. Passfeld [71], S.P. Pathak [124], R.N. Patra [137], B. Paul [58], H. Pei [7], T. Peitzmann [63], X. Peng [7], L.G. Pereira [73], H. Pereira Da Costa [75], D. Peresunko [83,90], E. Perez Lezama [70], V. Peskov [70], Y. Pestov [5], V. Petráček [39], V. Petrov [112], M. Petrovici [87], C. Petta [28], R.P. Pezzi [73], S. Piano [59], M. Pikna [38], P. Pillot [114], L.O.D.L. Pimentel [91], O. Pinazza [53,35], L. Pinsky [124], D.B. Piyarathna [124], M. Płoskoń [82], M. Planinic [98], F. Pliquett [70], J. Pluta [138], S. Pochybova [140], P.L.M. Podesta-Lerma [120], M.G. Poghosyan [95], B. Polichtchouk [112], N. Poljak [98], W. Poonsawat [115], A. Pop [87], H. Poppenborg [71], S. Porteboeuf-Houssais [131], V. Pozdniakov [77], S.K. Prasad [4], R. Preghenella [53], F. Prino [58], C.A. Pruneau [139], I. Pshenichnov [62], M. Puccio [26], V. Punin [108], J. Putschke [139], S. Raha [4], S. Rajput [101], J. Rak [125], A. Rakotozafindrabe [75], L. Ramello [32], F. Rami [133], D.B. Rana [124], R. Raniwala [102], S. Raniwala [102], S.S. Räsänen [46], B.T. Rascanu [70], D. Rathee [99], V. Ratza [45], I. Ravasenga [31], K.F. Read [127,95], K. Redlich [86,v], A. Rehman [22], P. Reichelt [70], F. Reidt [35], X. Ren [7], R. Renfordt [70], A. Reshetin [62], K. Reygers [104], V. Riabov [96], T. Richert [34,63], M. Richter [21], P. Riedler [35], W. Riegler [35], F. Riggi [28], C. Ristea [68], M. Rodríguez Cahuantzi [2], K. Røed [21], E. Rogochaya [77], D. Rohr [35,42], D. Röhrich [22], P.S. Rokita [138], F. Ronchetti [51], E.D. Rosas [72], P. Rosnet [131], A. Rossi [29,56], A. Rotondi [134], F. Roukoutakis [85], C. Roy [133], P. Roy [109], A.J. Rubio Montero [10], O.V. Rueda [72], R. Rui [25], B. Rumyantsev [77], A. Rustamov [89], E. Ryabinkin [90], Y. Ryabov [96], A. Rybicki [118], S. Saarinen [46], S. Sadhu [137], S. Sadovsky [112], K. Šafařík [35], S.K. Saha [137], B. Sahlmuller [70], B. Sahoo [48], P. Sahoo [49], R. Sahoo [49], S. Sahoo [67], P.K. Sahu [67], J. Saini [137], S. Sakai [130], M.A. Saleh [139], J. Salzwedel [18], S. Sambyal [101], V. Samsonov [96,83], A. Sandoval [74], A. Sarkar [76], D. Sarkar [137], N. Sarkar [137], P. Sarma [44], M.H.P. Sas [63], E. Scapparone [53], F. Scarlassara [29], B. Schaefer [95], H.S. Scheid [70], C. Schiaua [87], R. Schicker [104], C. Schmidt [106], H.R. Schmidt [103], M.O. Schmidt [104], M. Schmidt [103], N.V. Schmidt [95,70], J. Schukraft [35], Y. Schutz [35,133], K. Schwarz [106], K. Schweda [106], G. Scioli [27], E. Scomparin [58], M. Šefčík [40], J.E. Seger [97], Y. Sekiguchi [129], D. Sekihata [47], I. Selyuzhenkov [106,83], K. Senosi [76], S. Senyukov [133], E. Serradilla [74,10], P. Sett [48], A. Sevcenco [68], A. Shabanov [62], A. Shabetai [114], R. Shahoyan [35], W. Shaikh [109], A. Shangaraev [112], A. Sharma [99], A. Sharma [101], M. Sharma [101], M. Sharma [101], N. Sharma [99], A.I. Sheikh [137], K. Shigaki [47], S. Shirinkin [64], Q. Shou [7], K. Shtejer [9,26], Y. Sibiriak [90], S. Siddhanta [54], K.M. Sielewicz [35], T. Siemiarczuk [86], S. Silaeva [90], D. Silvermyr [34], G. Simatovic [92], G. Simonetti [35], R. Singaraju [137], R. Singh [88], V. Singhal [137], T. Sinha [109], B. Sitar [38], M. Sitta [32], T.B. Skaali [21], M. Slupecki [125], N. Smirnov [141], R.J.M. Snellings [63], T.W. Snellman [125], J. Song [19], M. Song [142], F. Soramel [29], S. Sorensen [127], F. Sozzi [106], I. Sputowska [118], J. Stachel [104], I. Stan [68], P. Stankus [95], E. Stenlund [34], D. Stocco [114], M.M. Storetvedt [37], P. Strmen [38], A.A.P. Suaide [121], T. Sugitate [47], C. Suire [61], M. Suleymanov [15], M. Suljic [25], R. Sultanov [64], M. Šumbera [94], S. Sumowidagdo [50], K. Suzuki [113], S. Swain [67], A. Szabo [38], I. Szarka [38], U. Tabassam [15], J. Takahashi [122], G.J. Tambave [22], N. Tanaka [130], M. Tarhini [61], M. Tariq [17], M.G. Tarzila [87], A. Tauro [35], G. Tejeda Muñoz [2], A. Telesca [35], K. Terasaki [129], C. Terrevoli [29], B. Teyssier [132], D. Thakur [49], S. Thakur [137], D. Thomas [119], F. Thoresen [91], R. Tieulent [132], A. Tikhonov [62], A.R. Timmins [124], A. Toia [70], M. Toppi [51], S.R. Torres [120], S. Tripathy [49], S. Trogolo [26], G. Trombetta [33], L. Tropp [40], V. Trubnikov [3], W.H. Trzaska [125], B.A. Trzeciak [63], T. Tsuji [129], A. Tumkin [108], R. Turrisi [56], T.S. Tveter [21], K. Ullaland [22], E.N. Umaka [124], A. Uras [132], G.L. Usai [24], A. Utrobicic [98], M. Vala [116,65], J. Van Der Maarel [63], J.W. Van Hoorne [35], M. van Leeuwen [63], T. Vanat [94], P. Vande Vyvre [35], D. Varga [140], A. Vargas [2], M. Vargyas [125], R. Varma [48], M. Vasileiou [85], A. Vasiliev [90], A. Vauthier [81], O. Vázquez Doce [105,36], V. Vechernin [136], A.M. Veen [63], A. Velure [22], E. Vercellin [26], S. Vergara Limón [2], R. Vernet [8], R. Vértesi [140], L. Vickovic [117], S. Vigolo [63], J. Viinikainen [125], Z. Vilakazi [128], O. Villalobos Baillie [110], A. Villatoro Tello [2], A. Vinogradov [90], L. Vinogradov [136], T. Virgili [30], V. Vislavicius [34], A. Vodopyanov [77], M.A. Völkl [103], K. Voloshin [64], S.A. Voloshin [139], G. Volpe [33], B. von Haller [35], I. Vorobyev [105,36], D. Voscek [116], D. Vranic [35,106], J. Vrláková [40], B. Wagner [22], H. Wang [63], M. Wang [7], D. Watanabe [130], Y. Watanabe [129,130], M. Weber [113], S.G. Weber [106], D.F. Weiser [104], S.C. Wenzel [35], J.P. Wessels [71], U. Westerhoff [71], A.M. Whitehead [100], J. Wiechula [70], J. Wikne [21], G. Wilk [86], J. Wilkinson [104,53], G.A. Willems [35,71], M.C.S. Williams [53], E. Willsher [110], B. Windelband [104], W.E. Witt [127], R. Xu [7], S. Yalcin [80], K. Yamakawa [47], P. Yang [7], S. Yano [47], Z. Yin [7], H. Yokoyama [130,81], I.-K. Yoo [19], J.H. Yoon [60], E. Yun [19], V. Yurchenko [3], V. Zaccolo [58], A. Zaman [15], C. Zampolli [35], H.J.C. Zanoli [121], N. Zardoshti [110], A. Zarochentsev [136], P. Závada [66], N. Zaviyalov [108], H. Zbroszczyk [138], M. Zhalov [96], H. Zhang [22,7], X. Zhang [7], Y. Zhang [7], C. Zhang [63], Z. Zhang [7,131], C. Zhao [21], N. Zhigareva [64], D. Zhou [7], Y. Zhou [91], Z. Zhou [22], H. Zhu [22], J. Zhu [7], Y. Zhu [7], A. Zichichi [12,27], M.B. Zimmermann [35], G. Zinovjev [3], J. Zmeskal [113], S. Zou [7]

[1] A.I. Alikhanyan National Science Laboratory (Yerevan Physics Institute) Foundation, Yerevan, Armenia
[2] Benemérita Universidad Autónoma de Puebla, Puebla, Mexico
[3] Bogolyubov Institute for Theoretical Physics, Kiev, Ukraine
[4] Bose Institute, Department of Physics and Centre for Astroparticle Physics and Space Science (CAPSS), Kolkata, India
[5] Budker Institute for Nuclear Physics, Novosibirsk, Russia
[6] California Polytechnic State University, San Luis Obispo, CA, United States
[7] Central China Normal University, Wuhan, China
[8] Centre de Calcul de l'IN2P3, Villeurbanne, Lyon, France
[9] Centro de Aplicaciones Tecnológicas y Desarrollo Nuclear (CEADEN), Havana, Cuba
[10] Centro de Investigaciones Energéticas Medioambientales y Tecnológicas (CIEMAT), Madrid, Spain
[11] Centro de Investigación y de Estudios Avanzados (CINVESTAV), Mexico City and Mérida, Mexico
[12] Centro Fermi – Museo Storico della Fisica e Centro Studi e Ricerche 'Enrico Fermi', Rome, Italy
[13] Chicago State University, Chicago, IL, United States
[14] China Institute of Atomic Energy, Beijing, China
[15] COMSATS Institute of Information Technology (CIIT), Islamabad, Pakistan
[16] Departamento de Física de Partículas and IGFAE, Universidad de Santiago de Compostela, Santiago de Compostela, Spain
[17] Department of Physics, Aligarh Muslim University, Aligarh, India
[18] Department of Physics, Ohio State University, Columbus, OH, United States
[19] Department of Physics, Pusan National University, Pusan, Republic of Korea
[20] Department of Physics, Sejong University, Seoul, Republic of Korea
[21] Department of Physics, University of Oslo, Oslo, Norway
[22] Department of Physics and Technology, University of Bergen, Bergen, Norway
[23] Dipartimento di Fisica dell'Università 'La Sapienza' and Sezione INFN, Rome, Italy
[24] Dipartimento di Fisica dell'Università and Sezione INFN, Cagliari, Italy
[25] Dipartimento di Fisica dell'Università and Sezione INFN, Trieste, Italy
[26] Dipartimento di Fisica dell'Università and Sezione INFN, Turin, Italy
[27] Dipartimento di Fisica e Astronomia dell'Università and Sezione INFN, Bologna, Italy
[28] Dipartimento di Fisica e Astronomia dell'Università and Sezione INFN, Catania, Italy
[29] Dipartimento di Fisica e Astronomia dell'Università and Sezione INFN, Padova, Italy
[30] Dipartimento di Fisica 'E.R. Caianiello' dell'Università and Gruppo Collegato INFN, Salerno, Italy
[31] Dipartimento DISAT del Politecnico and Sezione INFN, Turin, Italy
[32] Dipartimento di Scienze e Innovazione Tecnologica dell'Università del Piemonte Orientale and INFN Sezione di Torino, Alessandria, Italy
[33] Dipartimento Interateneo di Fisica 'M. Merlin' and Sezione INFN, Bari, Italy
[34] Division of Experimental High Energy Physics, University of Lund, Lund, Sweden
[35] European Organization for Nuclear Research (CERN), Geneva, Switzerland
[36] Excellence Cluster Universe, Technische Universität München, Munich, Germany
[37] Faculty of Engineering, Bergen University College, Bergen, Norway
[38] Faculty of Mathematics, Physics and Informatics, Comenius University, Bratislava, Slovakia
[39] Faculty of Nuclear Sciences and Physical Engineering, Czech Technical University in Prague, Prague, Czech Republic
[40] Faculty of Science, P.J. Šafárik University, Košice, Slovakia
[41] Faculty of Technology, Buskerud and Vestfold University College, Tonsberg, Norway
[42] Frankfurt Institute for Advanced Studies, Johann Wolfgang Goethe-Universität Frankfurt, Frankfurt, Germany
[43] Gangneung-Wonju National University, Gangneung, Republic of Korea
[44] Gauhati University, Department of Physics, Guwahati, India
[45] Helmholtz-Institut für Strahlen- und Kernphysik, Rheinische Friedrich-Wilhelms-Universität Bonn, Bonn, Germany
[46] Helsinki Institute of Physics (HIP), Helsinki, Finland
[47] Hiroshima University, Hiroshima, Japan
[48] Indian Institute of Technology Bombay (IIT), Mumbai, India
[49] Indian Institute of Technology Indore, Indore, India
[50] Indonesian Institute of Sciences, Jakarta, Indonesia
[51] INFN, Laboratori Nazionali di Frascati, Frascati, Italy
[52] INFN, Sezione di Bari, Bari, Italy
[53] INFN, Sezione di Bologna, Bologna, Italy
[54] INFN, Sezione di Cagliari, Cagliari, Italy
[55] INFN, Sezione di Catania, Catania, Italy
[56] INFN, Sezione di Padova, Padova, Italy
[57] INFN, Sezione di Roma, Rome, Italy
[58] INFN, Sezione di Torino, Turin, Italy
[59] INFN, Sezione di Trieste, Trieste, Italy
[60] Inha University, Incheon, Republic of Korea
[61] Institut de Physique Nucléaire d'Orsay (IPNO), Université Paris-Sud, CNRS-IN2P3, Orsay, France
[62] Institute for Nuclear Research, Academy of Sciences, Moscow, Russia
[63] Institute for Subatomic Physics of Utrecht University, Utrecht, Netherlands
[64] Institute for Theoretical and Experimental Physics, Moscow, Russia
[65] Institute of Experimental Physics, Slovak Academy of Sciences, Košice, Slovakia
[66] Institute of Physics, Academy of Sciences of the Czech Republic, Prague, Czech Republic
[67] Institute of Physics, Bhubaneswar, India
[68] Institute of Space Science (ISS), Bucharest, Romania
[69] Institut für Informatik, Johann Wolfgang Goethe-Universität Frankfurt, Frankfurt, Germany
[70] Institut für Kernphysik, Johann Wolfgang Goethe-Universität Frankfurt, Frankfurt, Germany
[71] Institut für Kernphysik, Westfälische Wilhelms-Universität Münster, Münster, Germany
[72] Instituto de Ciencias Nucleares, Universidad Nacional Autónoma de México, Mexico City, Mexico
[73] Instituto de Física, Universidade Federal do Rio Grande do Sul (UFRGS), Porto Alegre, Brazil
[74] Instituto de Física, Universidad Nacional Autónoma de México, Mexico City, Mexico
[75] IRFU, CEA, Université Paris-Saclay, Saclay, France
[76] iThemba LABS, National Research Foundation, Somerset West, South Africa
[77] Joint Institute for Nuclear Research (JINR), Dubna, Russia
[78] Konkuk University, Seoul, Republic of Korea
[79] Korea Institute of Science and Technology Information, Daejeon, Republic of Korea

[80] KTO Karatay University, Konya, Turkey
[81] Laboratoire de Physique Subatomique et de Cosmologie, Université Grenoble-Alpes, CNRS-IN2P3, Grenoble, France
[82] Lawrence Berkeley National Laboratory, Berkeley, CA, United States
[83] Moscow Engineering Physics Institute, Moscow, Russia
[84] Nagasaki Institute of Applied Science, Nagasaki, Japan
[85] National and Kapodistrian University of Athens, Physics Department, Athens, Greece
[86] National Centre for Nuclear Studies, Warsaw, Poland
[87] National Institute for Physics and Nuclear Engineering, Bucharest, Romania
[88] National Institute of Science Education and Research, HBNI, Jatni, India
[89] National Nuclear Research Center, Baku, Azerbaijan
[90] National Research Centre Kurchatov Institute, Moscow, Russia
[91] Niels Bohr Institute, University of Copenhagen, Copenhagen, Denmark
[92] Nikhef, Nationaal instituut voor subatomaire fysica, Amsterdam, Netherlands
[93] Nuclear Physics Group, STFC Daresbury Laboratory, Daresbury, United Kingdom
[94] Nuclear Physics Institute, Academy of Sciences of the Czech Republic, Řež u Prahy, Czech Republic
[95] Oak Ridge National Laboratory, Oak Ridge, TN, United States
[96] Petersburg Nuclear Physics Institute, Gatchina, Russia
[97] Physics Department, Creighton University, Omaha, NE, United States
[98] Physics department, Faculty of science, University of Zagreb, Zagreb, Croatia
[99] Physics Department, Panjab University, Chandigarh, India
[100] Physics Department, University of Cape Town, Cape Town, South Africa
[101] Physics Department, University of Jammu, Jammu, India
[102] Physics Department, University of Rajasthan, Jaipur, India
[103] Physikalisches Institut, Eberhard Karls Universität Tübingen, Tübingen, Germany
[104] Physikalisches Institut, Ruprecht-Karls-Universität Heidelberg, Heidelberg, Germany
[105] Physik Department, Technische Universität München, Munich, Germany
[106] Research Division and ExtreMe Matter Institute EMMI, GSI Helmholtzzentrum für Schwerionenforschung GmbH, Darmstadt, Germany
[107] Rudjer Bošković Institute, Zagreb, Croatia
[108] Russian Federal Nuclear Center (VNIIEF), Sarov, Russia
[109] Saha Institute of Nuclear Physics, Kolkata, India
[110] School of Physics and Astronomy, University of Birmingham, Birmingham, United Kingdom
[111] Sección Física, Departamento de Ciencias, Pontificia Universidad Católica del Perú, Lima, Peru
[112] SSC IHEP of NRC Kurchatov institute, Protvino, Russia
[113] Stefan Meyer Institut für Subatomare Physik (SMI), Vienna, Austria
[114] SUBATECH, IMT Atlantique, Université de Nantes, CNRS-IN2P3, Nantes, France
[115] Suranaree University of Technology, Nakhon Ratchasima, Thailand
[116] Technical University of Košice, Košice, Slovakia
[117] Technical University of Split FESB, Split, Croatia
[118] The Henryk Niewodniczanski Institute of Nuclear Physics, Polish Academy of Sciences, Cracow, Poland
[119] The University of Texas at Austin, Physics Department, Austin, TX, United States
[120] Universidad Autónoma de Sinaloa, Culiacán, Mexico
[121] Universidade de São Paulo (USP), São Paulo, Brazil
[122] Universidade Estadual de Campinas (UNICAMP), Campinas, Brazil
[123] Universidade Federal do ABC, Santo Andre, Brazil
[124] University of Houston, Houston, TX, United States
[125] University of Jyväskylä, Jyväskylä, Finland
[126] University of Liverpool, Liverpool, United Kingdom
[127] University of Tennessee, Knoxville, TN, United States
[128] University of the Witwatersrand, Johannesburg, South Africa
[129] University of Tokyo, Tokyo, Japan
[130] University of Tsukuba, Tsukuba, Japan
[131] Université CIermont Auvergne, CNRS/IN2P3, LPC, Clermont-Ferrand, France
[132] Université de Lyon, Université Lyon 1, CNRS/IN2P3, IPN-Lyon, Villeurbanne, Lyon, France
[133] Université de Strasbourg, CNRS, IPHC UMR 7178, F-67000 Strasbourg, France
[134] Università degli Studi di Pavia, Pavia, Italy
[135] Università di Brescia, Brescia, Italy
[136] V. Fock Institute for Physics, St. Petersburg State University, St. Petersburg, Russia
[137] Variable Energy Cyclotron Centre, Kolkata, India
[138] Warsaw University of Technology, Warsaw, Poland
[139] Wayne State University, Detroit, MI, United States
[140] Wigner Research Centre for Physics, Hungarian Academy of Sciences, Budapest, Hungary
[141] Yale University, New Haven, CT, United States
[142] Yonsei University, Seoul, Republic of Korea
[143] Zentrum für Technologietransfer und Telekommunikation (ZTT), Fachhochschule Worms, Worms, Germany

[i] Deceased.
[ii] Dipartimento DET del Politecnico di Torino, Turin, Italy.
[iii] M.V. Lomonosov Moscow State University, D.V. Skobeltsyn Institute of Nuclear, Physics, Moscow, Russia.
[iv] Department of Applied Physics, Aligarh Muslim University, Aligarh, India.
[v] Institute of Theoretical Physics, University of Wroclaw, Poland.